

Supporting Information S1

Through-Space Cation– π Quadrupole–Monopole Design Enables Selective Suppression of Third-Order Nonlinear Optical Kerr Effects

Daniels Jelisejevs^a, Arturs Bundulis^b, Anete Sapne^b, Kaspars Leduskrasts^{a*}

^aLatvian Institute of Organic Synthesis, Aizkraukles 21, LV-1006, Riga, Latvia

^bInstitute of Solid State Physics, University of Latvia, Kengaraga 8, LV-1063, Riga, Latvia

kledus@osi.lv

Contents

General considerations.....	2
Synthesis of NLO materials 1–5	3
Synthesis of 1a–c	3
Synthesis 2	6
Synthesis 3	8
Compound 4	9
Absorption in solution.....	10
Nonlinear optical measurements.....	12
DFT calculations.....	18
¹ H and ¹³ C NMR data.....	27

General considerations

Column chromatography was performed using reversed phase C18-silica gel columns (RP18 25-40 μm) and direct phase silica gel columns.

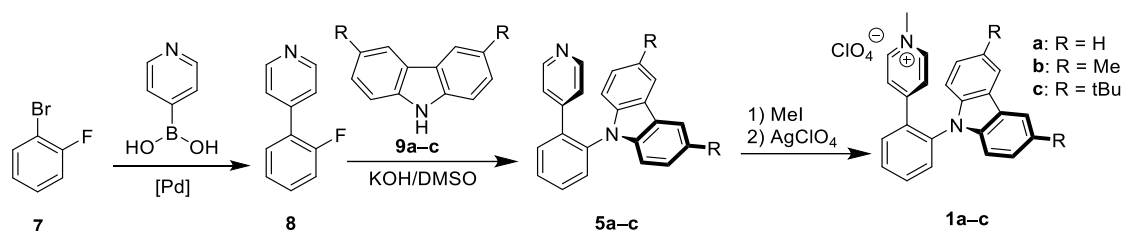
Nuclear magnetic resonance spectra were recorded on NMR spectrometers at the following frequencies: ^1H , 400 MHz, 300 MHz; $^{13}\text{C}\{^1\text{H}\}$, 101 MHz. Chemical shifts are reported in parts per million (ppm) relative to TMS or with the residual solvent peak as an internal reference. High-resolution mass spectra (HRMS (ESI-TOF)) were recorded on a mass spectrometer with a time-of-flight (TOF) mass analyzer using the ESI technique. Melting points are uncorrected.

Unless otherwise noted, all chemicals were used as received from commercial sources. Anhydrous THF was obtained by passing commercially available solvent through activated alumina columns.

The absorption data was collected with Edinburgh Instruments *FS5* Spectrofluorometer; NLO properties were characterized by Z-scan method using ORPHEUS-HP + PHAROS PH2 femtosecond laser with a repetition rate of 5 kHz to 500 kHz and pulse width of 150 fs was used as laser source.

Synthesis of NLO materials 1–5

Synthesis of 1a–c



4-(2-Fluorophenyl)pyridine (8). A 250 mL round bottom flask was charged with 1-bromo-2-fluorobenzene (**7**, 3.00 g, 17.1 mmol, 1.00 equiv), pyridine-4-boronic acid hydrate (3.62 g, 25.7 mmol, 1.50 equiv), potassium carbonate (7.10 g, 51.4 mmol, 3.00 equiv), Pd(dppf)Cl₂ × CH₂Cl₂ (0.70 g, 0.86 mmol, 0.05 equiv). Water (25 mL) and MeCN (140 mL) were added, and the mixture was stirred under reflux for 4h. After cooling to room temperature silica gel (5 g) was added and the solvent was removed under reduced pressure. The crude residue was dry loaded onto a silica column and purified using 100 % EtOAc as the mobile phase to obtain **8** as a red crystalline solid (2.87 g, 97%). The ¹H NMR was consistent with the previous report.¹

¹H NMR (300 MHz, acetone-*d*₆): δ 8.68 (dd, *J*=4.3, 1.7 Hz, 2H), 7.63 (dt, *J*=7.8, 1.7 Hz, 1H), 7.58–7.54 (m, 2H), 7.53–7.46 (m, 1H), 7.39–7.25 (m, 2H).

¹H NMR (400 MHz, CDCl₃, ppm) δ 8.68 (dd, *J*=4.6, 1.7 Hz, 2H), 7.52–7.34 (m, 4H), 7.30–7.14 (m, 2H).

¹³C {¹H} NMR (101 MHz, CDCl₃, ppm) δ 161.2, 158.7, 150.1, 143.6, 130.8 (*J*_F=8.4 Hz), 130.4 (*J*_F=3.1 Hz), 126.4 (*J*_F=12.7 Hz), 124.9 (*J*_F=3.6 Hz), 123.7 (*J*_F=3.4 Hz), 116.6 (*J*_F=22.3 Hz).

General method **A** for the synthesis of pyridines **5a–c**. 4-(2-Fluorophenyl)pyridine (**8**, 1.0 equiv), powdered KOH (10.0 equiv), respective carbazole (**9a–c**, 3.0 equiv), and DMSO (0.1 M) were combined and heated at 100 °C for 3 days under constant stirring. The cooled reaction mixture was diluted with water and extracted with EtOAc (3×50 mL). The combined organic phases were washed with water (3×30 mL) and brine (50 mL). The organic layers were dried over anhydrous Na₂SO₄, filtered, and concentrated under reduced pressure. Purification was carried out via silica gel column chromatography, using a 3:1 - Hexane:EtOAc as the mobile phase, to afford the desired carbazole derivatives (**1a–c**).

Supporting Information S4

Using general synthesis method **A** 9-(2-(pyridin-4-yl)phenyl)-9*H*-carbazole **5a** was obtained as a colorless crystalline solid (0.39 g, 48%); mp: 167–168 °C (EtOAc/Hexane).

¹H NMR (400 MHz, CDCl₃, ppm) δ 8.22 (dd, *J*=6.1, 1.7 Hz, 2H), 8.10–8.03 (m, 2H), 7.70–7.61 (m, 3H), 7.59–7.52 (m, 1H), 7.33–7.26 (m, 2H), 7.25–7.17 (m, 2H), 7.07–7.01 (m, 2H), 6.92 (dd, *J*=6.1, 1.6 Hz, 2H).

¹³C {¹H} NMR (101 MHz, CDCl₃, ppm) δ 149.8, 146.5, 141.1, 138.5, 135.1, 131.3, 130.4, 130.3, 129.3, 126.0, 123.3, 122.6, 120.4, 120.1, 109.8.

HR-MS (*m/z*) Calc. Mass for C₂₃H₁₇N₂⁺: 321.1392; Found: 321.1405.

IR (KBr, cm⁻¹) 1592 (C=C).

Using general synthesis method **A** 3,6-dimethyl-9-(2-(pyridin-4-yl)phenyl)-9*H*-carbazole **5b** was obtained as a white crystalline solid (0.35 g, 40%); mp: 164–166 °C (EtOAc/Hexane).

¹H NMR (400 MHz, CDCl₃, ppm) δ 8.23 (dd, *J*=6.0, 1.5 Hz, 2H), 7.84–7.78 (m, 2H), 7.68–7.58 (m, 3H), 7.55–7.49 (m, 1H), 7.11–7.08 (m, 1H), 7.08–7.04 (m, 1H), 6.93 (dd, *J*=6.0, 1.7 Hz, 2H), 6.91 (s, 1H), 6.89 (s, 1H), 2.48 (s, 6H).

¹³C {¹H} NMR (101 MHz, CDCl₃, ppm) δ 149.8, 146.7, 139.6, 138.3, 135.5, 131.2, 130.3, 130.2, 129.1, 129.0, 127.2, 123.3, 122.6, 120.3, 109.4, 21.5.

HR-MS (*m/z*) Calc. Mass for C₂₅H₂₁N₂⁺: 349.1705; Found: 349.1709.

IR (KBr, cm⁻¹) 1607 (C=C), 1487 (C–H).

Using general synthesis method **A** 3,6-di-*tert*-butyl-9-(2-(pyridin-4-yl)phenyl)-9*H*-carbazole **5c** was obtained as a white crystalline solid (0.40 g, 36%); mp: 157–159 °C (EtOAc/Hexane).

¹H NMR (400 MHz, CDCl₃, ppm) δ 8.30–8.23 (m, 2H), 8.09–8.04 (m, 2H), 7.70–7.56 (m, 3H), 7.51–7.46 (m, 1H), 7.35–7.30 (m, 2H), 7.00 (dd, *J*=6.1, 1.5 Hz, 2H), 6.95–6.93 (m, 1H), 6.93–6.91 (m, 1H), 1.42 (s, 18H).

¹³C {¹H} NMR (101 MHz, CDCl₃, ppm) δ 149.8, 146.8, 142.8, 139.7, 138.2, 135.7, 131.2, 130.3, 130.2, 128.9, 123.7, 123.4, 122.7, 116.4, 109.2, 34.8, 32.1.

HR-MS (*m/z*) Calc. Mass for C₃₁H₃₃N₂⁺: 433.2644; Found: 433.2652.

IR (KBr, cm⁻¹) 1592 (C=C), 1487 (C–H).

General method **B** for the synthesis of pyridinium salts **1a–c**. The corresponding pyridines (**5a–c**, 1.0 equiv) were dissolved in MeCN (10 mL) and MeI (5.0 equiv) was added. The reaction mixture was stirred at 40 °C for 3 days. To the cooled solution was added Et₂O and the precipitate filtered and washed with Et₂O. The precipitate was dissolved in MeCN (15

mL) and a solution of anhydrous AgClO_4 (1.2 equiv) in MeCN (5 mL) was added dropwise. After stirring for one hour at room temperature the suspension was filtered through a pad of celite, and the pad washed with MeCN. Most of the solvent was removed under reduced pressure and the resulting residue was recrystallized from *i*-PrOH/MeCN. The crystals were filtered, washed with *i*-PrOH and Et_2O , then dried in *vacuo* to give **1a–c**.

Using general synthesis method **B** 4-(2-(9*H*-carbazol-9-yl)phenyl)-1-methylpyridin-1-ium perchlorate **1a** was obtained as a yellow crystalline solid (0.26 g, 72%); mp. 138–140 °C (decomp.) (MeCN/*i*-PrOH).

$^1\text{H NMR}$ (600 MHz, CDCl_3 , ppm) δ 8.29 (d, $J=6.5$ Hz, 2H), 8.04 (d, $J=7.8$ Hz, 2H), 7.86–7.70 (m, 3H), 7.63–7.59 (m, 1H), 7.53–7.49 (m, 2H), 7.36–7.29 (m, 2H), 7.26–7.20 (m, 2H), 7.00 (d, $J=8.2$ Hz, 2H), 4.14 (s, 3H).

$^{13}\text{C } \{^1\text{H}\} \text{NMR}$ (151 MHz, CDCl_3 , ppm) δ 155.8, 144.8, 140.7, 135.3, 134.1, 133.4, 131.9, 130.5, 130.2, 126.8, 126.8, 123.5, 120.9, 120.8, 109.5, 48.3.

HR-MS (m/z) Calc. Mass for $\text{C}_{24}\text{H}_{19}\text{N}_2^+$: 335.1548. Found: 335.1559.

IR (KBr, cm^{-1}) 1641 (C=C), 1452 (C–H).

Using general synthesis method **B** 4-(2-(3,6-dimethyl-9*H*-carbazol-9-yl)phenyl)-1-methylpyridin-1-ium perchlorate **1b** was obtained as a yellow crystalline solid (0.25 g, 62%); mp. 236–238 °C (decomp.) (MeCN/*i*-PrOH).

$^1\text{H NMR}$ (400 MHz, CDCl_3 , ppm) δ 8.34–8.27 (m, 2H), 7.86–7.68 (m, 5H), 7.59 (dd, $J=7.8$, 1.3 Hz, 1H), 7.54–7.49 (m, 2H), 7.12 (ddd, $J=8.3$, 1.7, 0.7 Hz, 2H), 6.87 (s, 1H), 6.85 (s, 1H), 4.20 (s, 3H), 2.48 (s, 6H).

$^{13}\text{C } \{^1\text{H}\} \text{NMR}$ (101 MHz, CDCl_3 , ppm) δ 156.0, 144.7, 139.2, 135.8, 134.0, 133.4, 131.9, 130.5, 130.2, 129.9, 128.0, 126.7, 123.6, 120.7, 109.1, 48.3, 21.5.

HR-MS (m/z) Calc. Mass for $\text{C}_{26}\text{H}_{23}\text{N}_2^+$: 363.1861; Found: 363.1879.

IR (KBr, cm^{-1}) 1640 (C=C), 1463 (C–H).

Using general synthesis method **B** 4-(2-(3,6-di-*tert*-butyl-9*H*-carbazol-9-yl)phenyl)-1-methylpyridin-1-ium perchlorate **1c** was obtained as a yellow crystalline solid (0.32 g, 67%); mp. 291–293 °C (decomp.) (MeCN/*i*-PrOH).

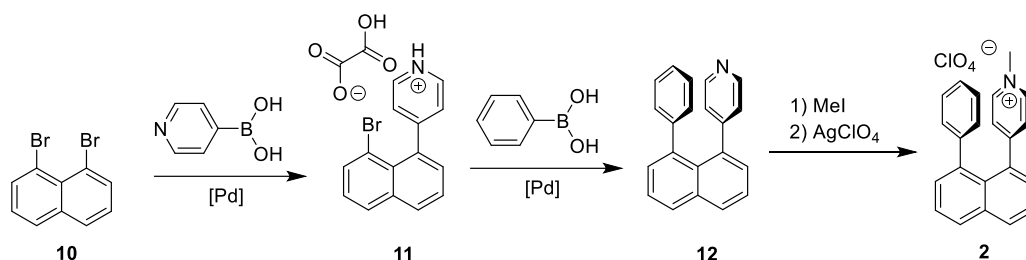
$^1\text{H NMR}$ (400 MHz, CDCl_3 , ppm) δ 8.38–8.33 (m, 2H), 8.06 (d, $J=1.9$ Hz, 2H), 7.86–7.82 (m, 1H), 7.79–7.68 (m, 2H), 7.61–7.53 (m, 3H), 7.38 (d, $J=1.9$ Hz, 1H), 7.35 (d, $J=1.9$ Hz, 1H), 6.90 (s, 1H), 6.88 (s, 1H), 4.22 (s, 3H), 1.42 (s, 18H).

^{13}C { ^1H } NMR (101 MHz, CDCl_3 , ppm) δ 156.1, 144.8, 143.9, 139.2, 136.0, 133.9, 133.4, 131.8, 130.5, 129.9, 126.8, 124.5, 123.6, 116.8, 108.9, 48.3, 34.9, 32.1.

HR-MS (m/z) Calc. Mass for $\text{C}_{32}\text{H}_{35}\text{N}_2^+$: 447.2800; Found: 447.2805.

IR (KBr, cm^{-1}) 1640 (C=C), 1490 (C-H).

Synthesis 2



4-(8-Bromonaphthalen-1-yl)pyridin-1-ium carboxyformate (11). 1,8-Dibromonaphthalene (**10**, 2.0 g, 7.0 mmol, 1.0 equiv), pyridine-4-boronic acid hydrate (0.84 g, 7.0 mmol, 1.0 equiv), $\text{Pd}(\text{dppf})\text{Cl}_2 \times \text{CH}_2\text{Cl}_2$ (0.29 g, 0.35 mmol, 0.05 equiv), K_2CO_3 (2.9 g, 21.0 mmol, 3.0 equiv) were weighed into a 100 mL round bottom flask. Acetonitrile (30 mL) and water (10 mL) were added and the resulting brown emulsion was refluxed for 2h. The reaction mixture was cooled, diluted with CH_2Cl_2 (50 mL) and sat. aq. K_2CO_3 (50 mL) solution. Layers were separated and the aqueous layer was extracted with CH_2Cl_2 (3 x 50 mL). Combined organic layers were dried over Na_2SO_4 , filtered and concentrated *in vacuo*. Purification of the residue by silica gel column chromatography using gradient elution from 10:1 to 3:1 Hexanes:EtOAc afforded a pale yellow amorphous material. The latter was dissolved in Et_2O (20 mL) and a solution of oxalic acid (0.64 g, 7.0 mmol, 1.0 equiv) in 20 mL Et_2O was added leading to formation of a colorless precipitate. The resulting suspension was filtered, washed with Et_2O and dried under vacuum to afford **11** as colorless needles (1.7 g, 65%); mp (MeCN/ Et_2O) 198–200 °C (colorless needles).

^1H NMR (400 MHz, CD_3OD , ppm) δ 8.77–8.70 (m, 2H), 8.12 (dd, $J=8.2, 1.2$ Hz, 1H), 8.07 (dd, $J=8.2, 1.2$ Hz, 1H), 7.89 (dd, $J=7.5, 1.2$ Hz, 1H), 7.84–7.79 (m, 2H), 7.68–7.61 (m, 1H), 7.52 (dd, $J=7.2, 1.2$ Hz, 1H), 7.49–7.43 (m, 1H).

^{13}C { ^1H } NMR (101 MHz, CD_3OD , ppm) δ 164.5, 159.4, 144.8, 144.7, 137.8, 137.0, 135.5, 132.8, 132.4, 130.6, 129.8, 128.6, 128.3, 126.7, 119.8.

IR (KBr, cm^{-1}) 2559 (O-H), 1711 (C=O).

HR-MS (m/z) Calc. Mass for $\text{C}_{15}\text{H}_{11}\text{BrN}^+$: 284.0069; Found: 284.0086.

4-(8-Phenyl-naphthalen-1-yl)pyridine (12). 4-(8-Bromonaphthalen-1-yl)pyridin-1-ium carboxyformate (**11**, 1.72 g, 4.6 mmol, 1.0 equiv), phenyl boronic acid (0.66 g, 5.5 mmol, 1.2 equiv), Pd(dppf)Cl₂ × CH₂Cl₂ (0.19 g, 0.2 mmol, 0.05 equiv), K₂CO₃ (1.90 g, 13.7 mmol, 3.0 equiv) were weighed into a 100 mL round bottom flask. MeCN (24 mL) and water (6 mL) were added to the flask and the resulting brown emulsion was refluxed. After 2h the reaction mixture was cooled and directly adsorbed on silica gel. Purification by silica gel column chromatography using gradient elution from 6:1 to 3:1 hexane:EtOAc afforded **12** as colorless plates (0.79 g, 62%). Analytical TLC on silica gel, 1:3 EtOAc/Hexanes, *R_f*=0.39, mp (hexane/EtOAc) 194–195 °C (colorless plates).

¹H NMR (400 MHz, CDCl₃, ppm) δ 8.17–8.12 (m, 2H), 8.01 (dd, *J*=8.2, 1.3 Hz, 1H), 7.98 (dd, *J*=8.2, 1.3 Hz, 1H), 7.63–7.54 (m, 2H), 7.46 (dd, *J*=7.0, 1.4 Hz, 1H), 7.37 (dd, *J*=7.0, 1.4 Hz, 1H), 7.06–6.94 (m, 5H), 6.89–6.85 (m, 2H).

¹³C{¹H} NMR (101 MHz, CDCl₃, ppm) δ 151.1, 148.6, 142.8, 140.1, 137.8, 135.5, 131.2, 131.1, 130.1, 129.9, 129.0, 128.8, 127.7, 126.8, 125.7, 125.2, 124.8.

IR (KBr, cm⁻¹) 1592 (C=C).

HR-MS (*m/z*) Calc. Mass for C₂₁H₁₆N⁺: 282.1283; Found: 282.1300.

1-Methyl-4-(8-phenyl-naphthalen-1-yl)pyridin-1-ium perchlorate (2). 4-(8-Phenyl-naphthalen-1-yl)pyridine (**12**, 0.79 g 2.8 mmol, 1.0 equiv) was dissolved in MeCN (30 mL) followed by addition of MeI (1.2 g, 8.4 mmol, 3.0 equiv), the vial sealed with septum and heated in a 70 °C oil bath for 2h. After cooling Et₂O was added to form precipitate, which was filtered, washed with Et₂O and redissolved in MeCN (25 mL). To the MeCN solution of the iodide salt a solution of AgClO₄ (0.75 g, 3.6 mmol, 1.3 equiv) in MeCN (5 mL) was added. The resulting suspension was stirred at room temperature for one hour, filtered through a pad of celite, and the pad was washed with MeCN. The filtrate was partially evaporated to roughly 5 mL volume, then diluted with *i*-PrOH (40 mL), evaporated again to approximately 5 mL volume and diluted with *i*-PrOH (40 mL) again, then sonified, and left to stand at -15 °C for 2h. The formed suspension was filtered and washed with *i*-PrOH to afford **2** as colorless plates (0.90 g, 81%); mp (*i*-PrOH/MeCN) 201–203°C (colorless plates).

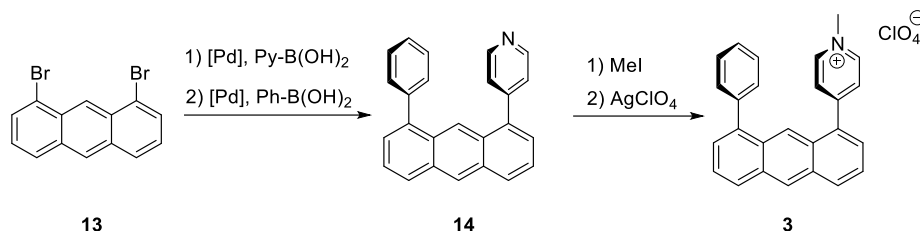
¹H NMR (400 MHz, (CD₃)₂SO, ppm) δ 8.41–8.37 (m 2H), 8.26 (dd, *J*=8.3, 1.2 Hz, 1H), 8.16 (dd, *J*=8.3, 1.2 Hz, 1H), 7.76–7.70 (m, 2H), 7.61–7.53 (m, 4H), 7.18–7.12 (m, 1H), 7.08–7.03 (m, 2H), 7.02–6.97 (m, 2H), 4.12 (s, 3H).

¹³C{¹H} NMR (101 MHz, (CD₃)₂SO, ppm) δ 158.9, 143.3, 142.3, 138.8, 135.2, 134.1, 132.2, 132.1, 131.6, 130.6, 129.5, 128.6, 128.2, 128.0, 127.0, 126.9, 125.9, 47.1.

IR (KBr, cm^{-1}) 1640 (C=C);

HR-MS (m/z) Calc. Mass for $\text{C}_{22}\text{H}_{18}\text{N}^+$: 296.1439; Found: 296.1436.

Synthesis 3.



4-(8-Phenylanthracen-1-yl)pyridine (14). 1,8-Dibromoanthracene (**13**, 100 mg, 0.30 mmol, 1.00 equiv), pyridine-4-boronic acid hydrate (36 mg, 0.29 mmol, 0.98 equiv), K_2CO_3 (123 mg, 0.89 mmol, 3.00 equiv) and $\text{Pd}(\text{dppf})\text{Cl}_2 \times \text{CH}_2\text{Cl}_2$ (12 mg, 0.015 mmol, 0.05 equiv) were combined in a 5 mL vial. Toluene (1.0 mL) and degassed water (0.10 mL) were added, the flask sealed and the formed suspension was stirred at room temperature. A stream of argon was passed through a vigorously stirred suspension for 10 minutes, and the formed suspension was stirred at 80 °C. After 16 h additional $\text{Pd}(\text{dppf})\text{Cl}_2 \times \text{DCM}$ (12 mg, 0.015 mmol, 0.05 equiv) and pyridine-4-boronic acid hydrate (7 mg, 0.060 mmol, 0.20 equiv) were added. Reaction mixture was stirred at 80 °C for 4h and then phenyl boronic acid (54 mg, 0.45 mmol, 1.50 equiv) and $\text{Pd}(\text{dppf})\text{Cl}_2 \times \text{DCM}$ (12 mg, 0.015 mmol, 0.05 equiv) were added and suspension was left to stir at 80 °C. After 16h reaction mixture was cooled to room temperature and concentrated on silica gel in *vacuo*. The residue was purified by column chromatography on silica gel using 30–100% of EtOAc in petroleum ether as the mobile phase. Compound **14** was obtained as an orange amorphous solid (40 mg, 41%).

¹H NMR (400 MHz, CDCl_3 , ppm) δ 8.65 (broad s, 2H), 8.57 (s, 1H), 8.53 (s, 1H), 8.14–8.01 (m, 2H), 7.61–7.50 (m, 2H), 7.49–7.34 (m, 9H).

¹³C {¹H} NMR (101 MHz, CDCl_3 , ppm) δ 149.7, 148.6, 140.7, 140.3, 137.8, 132.1, 131.8, 130.6, 130.0, 129.2, 129.1, 128.4, 127.8, 127.7, 127.3, 126.6, 126.6, 125.8, 125.2, 125.1, 123.3.

HR-MS (m/z) Calc. Mass for $\text{C}_{25}\text{H}_{18}\text{N}$: 332.1439. Found: 332.1448.

IR (KBr, cm^{-1}) 1593 (C=C).

1-Methyl-4-(8-phenylanthracen-1-yl)pyridinium perchlorate (3). To a solution of 4-(8-phenylanthracen-1-yl)pyridine (**14**; 75 mg, 0.23 mmol, 1.00 equiv) in anhydrous MeCN (1.5 mL) was added iodomethane (0.04 mL, 0.54 mmol, 2.40 equiv) and the resulting colorless

solution was stirred in a pressure vial at 70 °C. After 2h the solution was evaporated and the resulting iodide salt was dissolved in MeCN (1.5 mL). To the MeCN solution of the iodide salt a solution of AgClO₄ (50 mg, 0.241 mmol, 1.20 equiv) in MeCN (1.0 mL) was added dropwise. The resulting suspension was stirred at room temperature for 1h, then filtered through a pad of Celite and the pad was washed with MeCN. The filtrate was evaporated to give orange solid which was crystallized from MeCN/*i*-PrOH, then left to stand at -15 °C overnight, filtered, washed with *i*-PrOH and dried to afford the title compound **3** as an orange powder (68 mg, 76%); mp 208–210 °C (MeCN/*i*-PrOH).

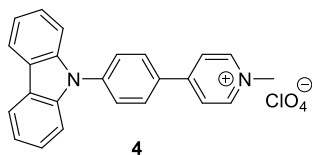
¹H NMR (400 MHz, (CD₃)₂SO, ppm) δ 9.13–9.07 (m, 2H), 8.89 (s, 1H), 8.52–8.42 (m, 3H), 8.42–8.34 (m, 1H), 8.22 (d, *J*=8.6 Hz, 1H), 7.76–7.65 (m, 5H), 7.64–7.53 (m, 3H), 7.49–7.42 (m, 1H), 4.40 (s, 3H).

¹³C {¹H} NMR (101 MHz, (CD₃)₂SO, ppm) δ 155.6, 145.4, 139.6, 139.5, 133.8, 131.9, 131.5, 131.1, 130.1, 129.8, 129.3, 128.7, 128.3, 128.0, 128.0, 127.9, 127.4, 127.3, 126.4, 125.5, 121.4, 47.6.

HR-MS (*m/z*) Calc. Mass for C₂₆H₂₀N⁺: 346.1596. Found: 346.1604.

IR (KBr, cm⁻¹) 1638 (C=C).

Compound 4.



4-(4-(9H-Carbazol-9-yl)phenyl)-1-methylpyridin-1-ium (4) was synthesized according to previously published protocol and the ¹H NMR was consistent with previous report.²

¹H NMR (400 MHz, (CD₃)₂SO, ppm) δ 9.00–8.95 (m, 2H), 8.56–8.50 (m, 2H), 8.37–8.31 (m, 2H), 8.29–8.23 (m, 2H), 7.94–7.88 (m, 2H), 7.54–7.45 (m, 4H), 7.36–7.29 (m, 2H), 4.34 (s, 3H).

Absorption in solution

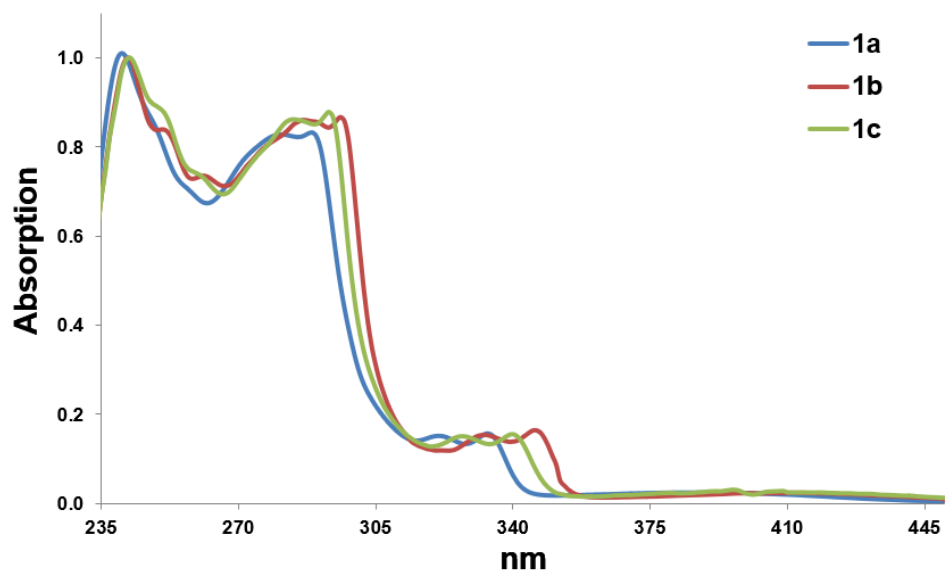


Fig. S1. Absorption of **1a–c** in MeCN solution (at 10^{-5} mol/L)

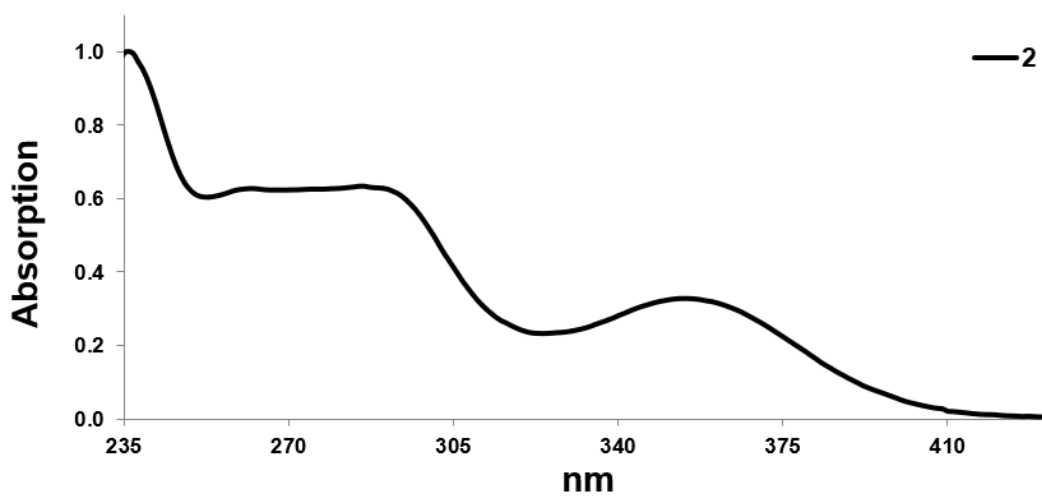


Fig. S2. Absorption of **2** in MeCN solution (at 10^{-5} mol/L)

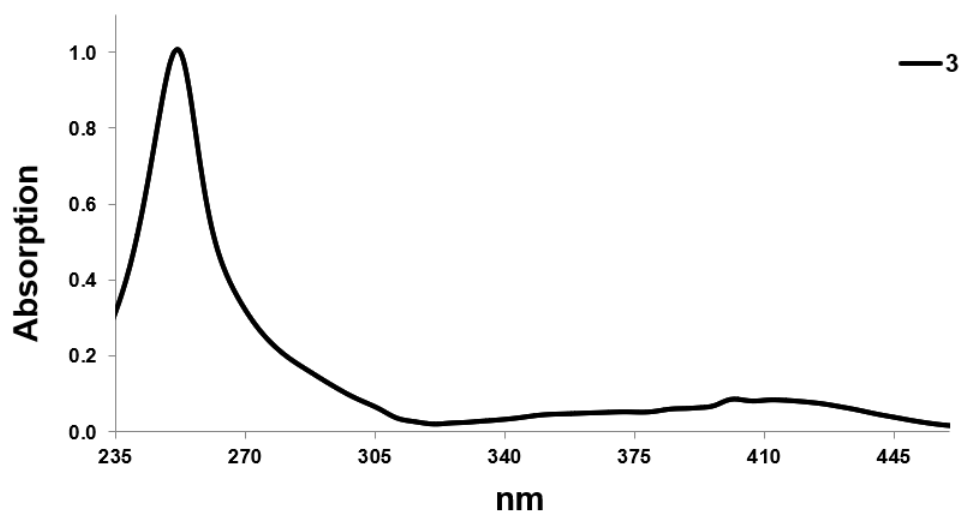


Fig. S3. Absorption of **3** in MeCN solution (at 10^{-5} mol/L)

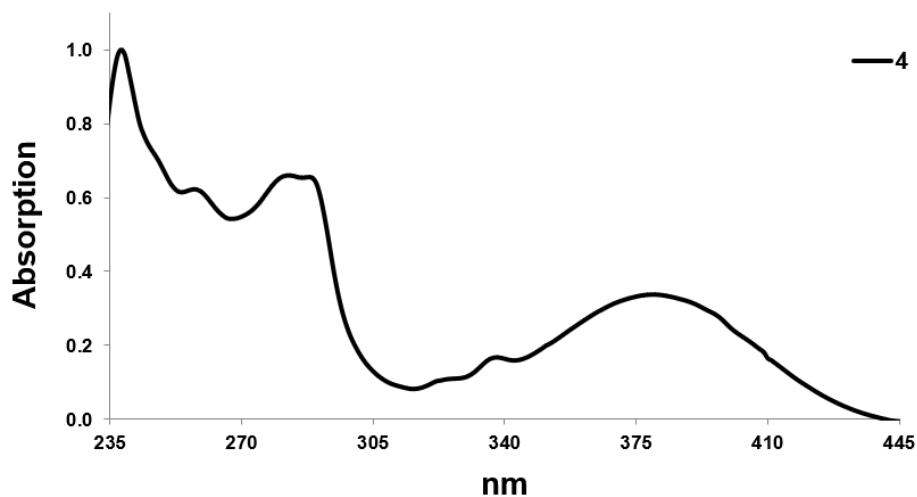


Fig. S4. Absorption of **4** in MeCN solution (at 10^{-5} mol/L)

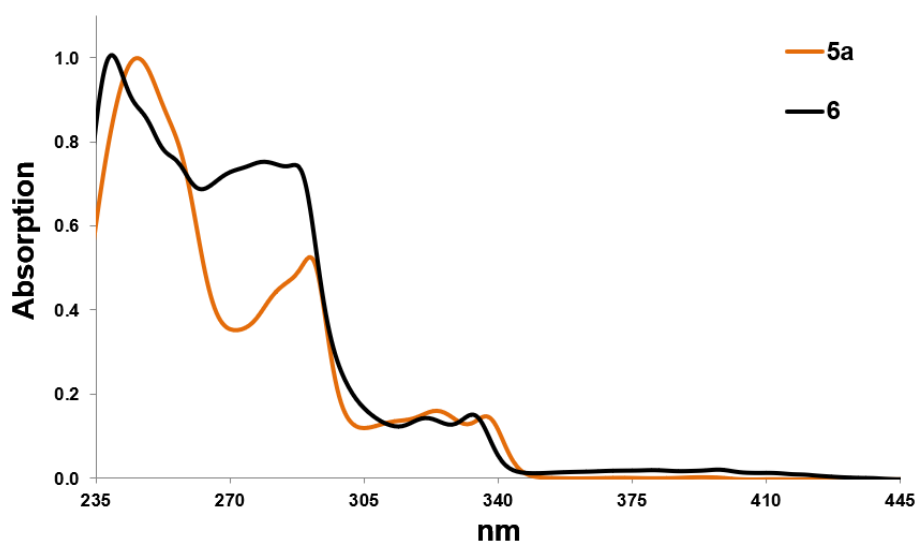


Fig. S5. Absorption of **5a** and **6** in MeCN solution (at 10^{-5} mol/L)

Nonlinear optical measurements

In this study, NLO properties were characterized using the Z-scan method.³ Compared to other NLO characterization methods, Z-scan method has a very simple experimental setup and data fitting as well as it allows to simultaneously measure both nonlinear refractive index and absorption changes. During measurement sample was moved through focused laser beam and the transmitted signal is detected using two detectors – open-aperture measurement that measures overall power and is influenced by absorption changes and closed-aperture measurement where small pinhole is placed in front of detector to measure signal intensity changes that is influenced by both absorption and refractive index changes.

For experimental measurements a tuneable ORPHEUS-HP + PHAROS PH2 femtosecond laser with a repetition rate of 5 kHz to 500 kHz and pulse width of 150 fs was used as laser source, to ensure that no thermal or molecular reorientation effects would influence measurements as pulse width was too short. To focus the laser beam, a lens with a focal length of 110 mm was used, resulting in a calculated Rayleigh length of 1.2 mm for this experimental setup.

Open-aperture measurements for Two-photon absorption can be fitted using standard Z-scan equation (eq. 1):³

$$T_{OA} = \sum_{k=0}^{\infty} \frac{\left(\frac{q}{1 + \frac{z^2}{z_R^2}} \right)^k}{(k+1)^{3/2}} \quad (1)$$

where $q = \alpha_2 \cdot I \cdot L_{\text{eff}}$, I is optical intensity, $L_{\text{eff}} = (1 - \exp(-\alpha_0 \cdot L)) / \alpha_0$ is effective length, α_0 is optical absorption, L is thickness, z is sample position and z_R is Rayleigh length. To study Kerr effect the closed-aperture measurements are divided by open aperture measurements.

Resulting data for third-order Kerr effect can be fitted using equation (eq. 2):³

$$T_{CA} = 1 + \frac{4 \cdot \Delta\Phi \cdot \frac{z}{z_R}}{\left(\frac{z^2}{z_R^2} + 9 \right) \left(\frac{z^2}{z_R^2} + 1 \right)} + \frac{4 \left(3 \frac{z^2}{z_R^2} - 5 \right) \Delta\Phi_{01}^2}{\left(\frac{z^2}{z_R^2} + 1 \right)^2 \left(\frac{z^2}{z_R^2} + 9 \right) \left(\frac{z^2}{z_R^2} + 25 \right)}, \quad (2)$$

Where $\Delta\Phi = n_2 \cdot k \cdot I \cdot L_{\text{eff}}$ is induced phase change, n_2 is Kerr coefficient and k is wave number.

In general, the $(2m + 1)$ -th order nonlinear induced phase change can be expressed as (eq. 3):

$$\Delta\Phi_{0m} = k \cdot n_{2m} \cdot I^m \cdot L, \quad (3)$$

In case if both 5th and 3rd order effects are observed simultaneously, both their contributions to transmittance were taken in account in form (eq. 4 and 5):

$$T_1(\Delta\Phi_{01}) = 1 + \frac{4\frac{z}{z_R}\Delta\Phi_{01}}{\left(\frac{z^2}{z_R^2}+1\right)^2\left(\frac{z^2}{z_R^2}+9\right)} + \frac{4\left(3\frac{z^2}{z_R^2}-5\right)\Delta\Phi_{01}^2}{\left(\frac{z^2}{z_R^2}+1\right)^2\left(\frac{z^2}{z_R^2}+9\right)\left(\frac{z^2}{z_R^2}+25\right)}, \quad (4)$$

$$T_2(\Delta\Phi_{02}) = 1 + \frac{8\frac{z}{z_R}\Delta\Phi_{02}}{\left(\frac{z^2}{z_R^2}+1\right)^2\left(\frac{z^2}{z_R^2}+25\right)} + \frac{48\left(\frac{z^2}{z_R^2}-3\right)\Delta\Phi_{02}^2}{\left(\frac{z^2}{z_R^2}+1\right)^4\left(\frac{z^2}{z_R^2}+25\right)\left(\frac{z^2}{z_R^2}+81\right)}, \quad (5)$$

Additionally, a mixing term of both effects needs to be taken in account giving the final equation of form (eq. 6):

$$T(\Delta\Phi_{01}, \Delta\Phi_{02}) = T_1(\Delta\Phi_{01}) + T_2(\Delta\Phi_{02}) - 1 + \frac{48\Delta\Phi_{01}\Delta\Phi_{02}\left(\frac{z^4}{z_R^4}+14\frac{z^2}{z_R^2}-35\right)}{\left(\frac{z^2}{z_R^2}+1\right)^3\left(\frac{z^2}{z_R^2}+9\right)\left(\frac{z^2}{z_R^2}+25\right)\left(\frac{z^2}{z_R^2}+49\right)}, \quad (6)$$

Measured samples were contained in quartz cuvette with 1mm optical path. For reference measurements pure MeCN was used.

To verify that the observed NLO effect corresponded to a fifth-order process, the measured phase change was plotted as a function of laser power to determine whether the dependence was linear or quadratic. As shown in Figure S6, the phase change measured for pure MeCN and compound **2** demonstrates that MeCN exhibits a linear dependence consistent with a third-order effect, whereas compound **2** shows a quadratic dependence characteristic of a fifth-order effect.

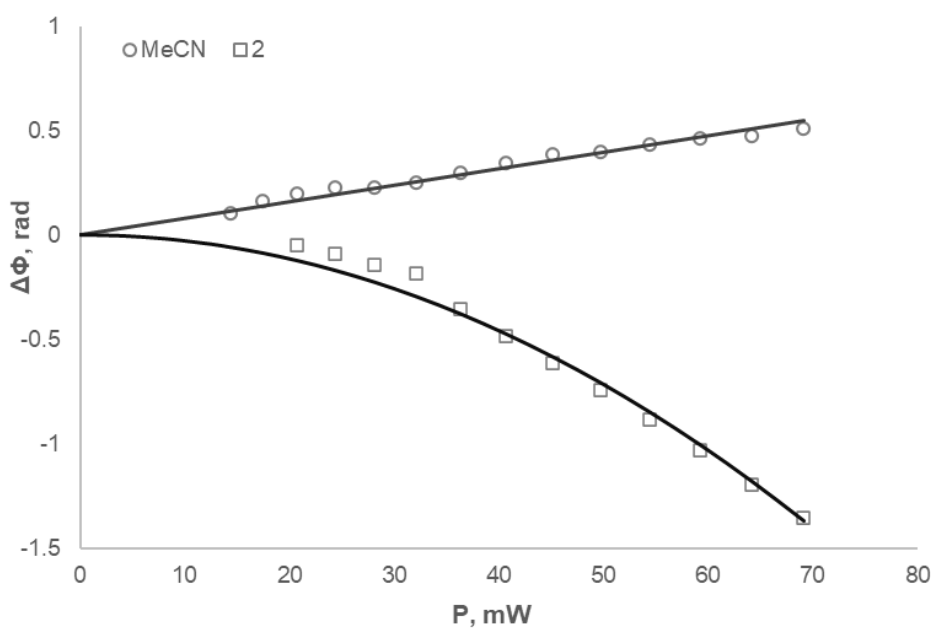


Fig. S6. Phase change power dependence for MeCN and **2**.

To convert third-order NLO effect coefficients (Kerr coefficient and Two-photon absorption coefficient) the following equations were used (eq. 7):

$$\begin{cases} \chi_{Re}^{(3)} = \frac{4 \cdot n_0^2 \cdot \epsilon_0 \cdot c}{3} \cdot n_2 \\ \chi_{Im}^{(3)} = \frac{\lambda \cdot n_0^2 \cdot \epsilon_0 \cdot c}{3 \cdot \pi} \cdot \alpha_2 \end{cases} \quad (7)$$

Where n_0 is refractive index, c is speed of lights and ϵ_0 is vacuum permittivity. In case of fifth-order NLO effects only the real part of fifth-order dielectric susceptibility was calculated using (eq. 8):

$$\chi_{Re}^{(5)} = \frac{4 \cdot n_0^3 \cdot \epsilon_0^2 \cdot c^2}{5} \cdot n_4 \quad (8)$$

To study the nonlinear refractive properties on molecular level third- and fifth- order dielectric susceptibilities were converted to second- and forth- order hyperpolarizability, respectively. Conversion was done using the following formulas (eq. 9):

$$\begin{cases} \gamma = \frac{\chi_{Re}^{(3)}}{N \cdot L^4} \\ \varepsilon = \frac{\chi_{Re}^{(5)}}{N \cdot L^6} \end{cases} \quad (9)$$

where N is molecule concentration per cm^3 and L is local field factor.

Measurements of n_4 at 500 kHz in 800–900 nm spectral range showed a strong dependence on wavelength with all compounds n_4 decreasing for longer wavelengths (see Figure S7).

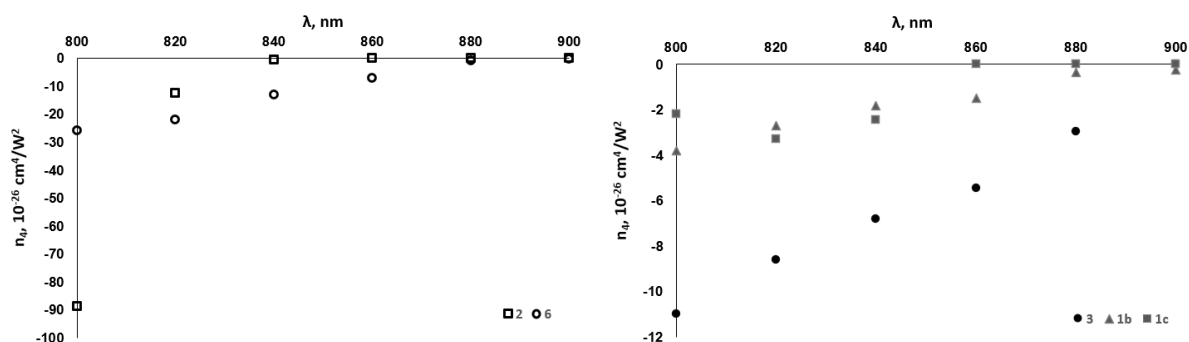


Fig. S7. The n_4 at 500 kHz in the 800–900 nm range for **1b**, **1c**, **2**, **3**, and **6**.

When measurements were carried out at 5 kHz the n_4 values were close to zero with only compound **2** exhibiting modest $n_4 = -2.25 \cdot 10^{-26} \text{ cm}^4/\text{W}^2$ at 800 nm (see *Table S1*).

Table S1. The n_4 values for **1b**, **1c**, **2**, **3**, and **6** at 800 nm (5 kHz repetition rate).

Compound	n_4 , $10^{-26} \text{ cm}^4/\text{W}^2$
1b	-
1c	-
2	-2.25
3	-
6	-

To further probe the origin of the fifth-order nonlinear refraction response polarization-resolved Z-scan was utilized (see below).

Background: Z-scan technique can be enhanced for a more detailed investigation of nonlinear optical (NLO) properties with polarization-resolved measurement. By adjusting the polarization state of the incident laser beam using a $\lambda/4$ waveplate within the Z-scan setup, it becomes possible to probe the physical mechanisms underlying the nonlinear response.⁴ This approach has been successfully applied to a range of systems, including CS_2 ,^{5,6} various organic solvents,⁷ and organic dyes,^{8,9} demonstrating both its experimental simplicity and its ability to provide insights beyond standard Z-scan measurements. Polarization-resolved Z-scan has predominantly been employed to study third-order nonlinearities, but its extension to fifth-order effects could offer a deeper understanding of the origins of nonlinear behaviour. In contrast to frequency-dependent techniques,¹⁰ polarization-dependent measurements not only enable the separation of thermal and nonlinear optical contributions but also provide additional information about the fundamental mechanisms driving the nonlinear response.

Methodology: The Kerr coefficient can be expressed as a fourth-order tensor of third-order susceptibility. For isotropic media the tensor has only two independent components - χ_{xxyy} and χ_{xyyx} . Depending on incident lights polarization the contribution of each of these elements to overall response varies and can be expressed as:

$$n_2 = \pi \cdot (12 \cdot \chi_{xxyy} + 6 \cdot \chi_{xyyx} \cdot (\sin 2\theta)^2) \cdot \frac{|E|^2}{n_0}$$

where θ is the angle between $\lambda/4$ plate slow axis and the laser beam polarization direction, and E is the electrical field amplitude. The ratio of $r = \chi_{xyyx}/\chi_{xxyy}$ can be used to study the origins of NLO response with:

- $r=6$ indicating that molecular reorientation causes refractive index variation;
- $r=1$ indicating the electronic response dominant;
- for $r=0$ thermo-optical effect is the dominant process in case of third-order Kerr effect.⁴

Results: The decrease of n_4 value with pulse repetition rate indicates that n_4 could be due to thermal effects induced by two-photon absorption (see above). To study the origin of the

observed fifth-order nonlinear refraction in more detail, polarization resolved Z-scan measurements were carried out.

The induced phase change for acetonitrile and **1b** is shown in Figure S8. It can be observed that for both compounds the phase change decrease for circular polarization with r values of $r=2.03$ for acetonitrile and $r=1.49$ for **1b**. From theory in case of thermal effects no polarization dependence should be observed. The observed r value for **1b** provides strong evidence against the thermo-optical effect and indicates that the observed negative nonlinear refractive index is of Kerr origins. As there is no theory of polarization resolved measurements of fifth-order effects for Z-scan, it is difficult to assess how much of it is reorientation or electronic effect.

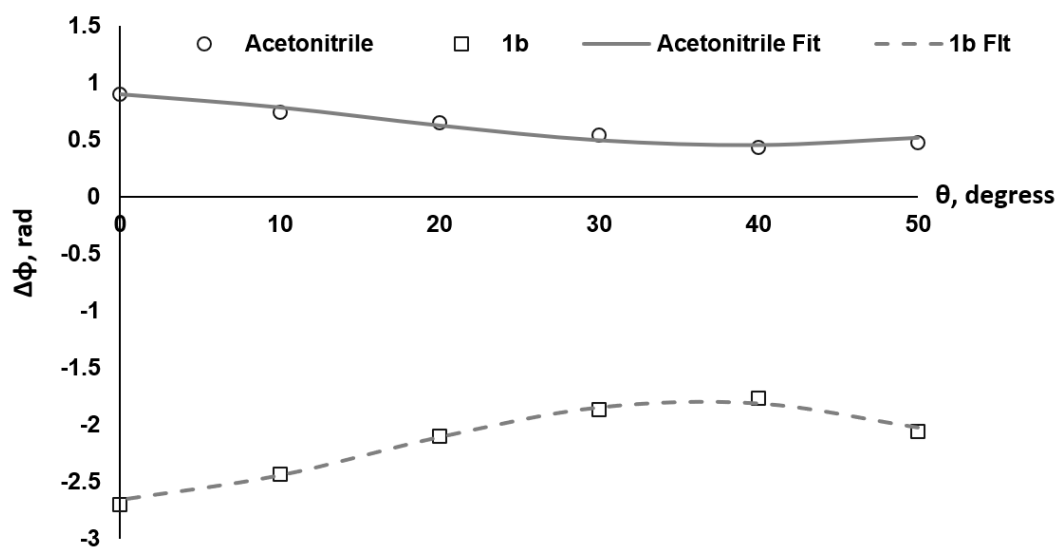
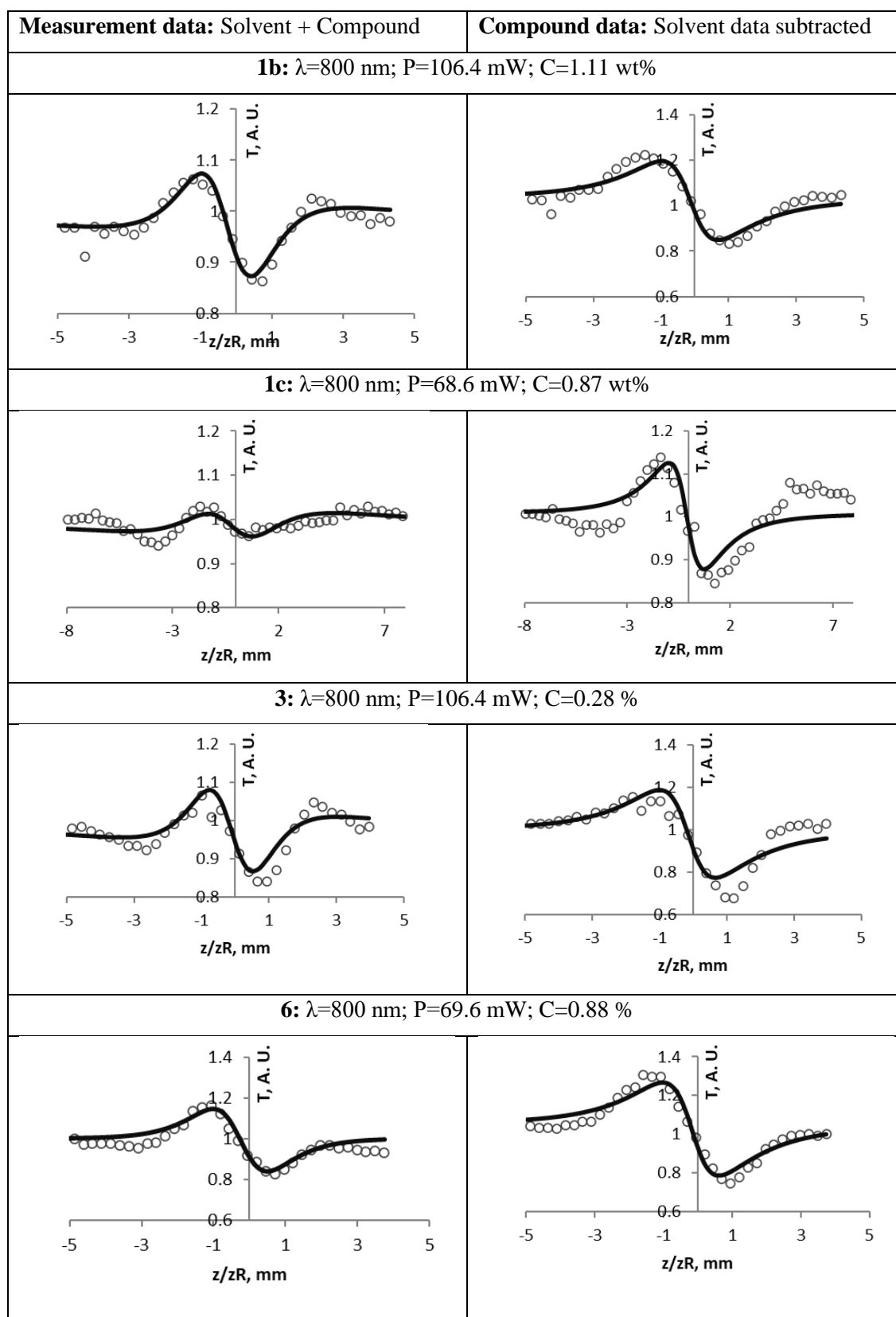


Fig. S8. Polarization-resolved Z-scan measurements at 800 nm for **1b**.

The solvent's third- and material's fifth-order effects mix for **1b**, **1c**, **3**, and **6** are shown in Table S2, including measurement information (wavelength, laser power and compound concentration). Graphs for compound solution measurements containing both solvent third-order effect and fifth-order effect of the compound, as well as the isolated compound fifth-order signal acquired by subtracting solvent signal from solution signal.

Table S2: Measurement examples of all compounds.



DFT calculations

Computational Details. All density functional theory (DFT) calculations were performed using the Gaussian 09 suite of programs. The computational workflow for evaluating the induced dipole moments (μ_{ind}) consisted of the following steps:

1) Geometry Optimization and Frequency Calculations. Initial geometry optimizations of the molecules and their isolated fragments were carried out utilizing the ω B97X-D functional, which inherently accounts for long-range dispersion interactions, paired with the def2-SVP basis set. An ultrafine integration grid (integral=ultrafine) was employed to ensure numerical accuracy and stability during the optimization process. Force constants were calculated at the first step (calcfc), and subsequent vibrational frequency analyses confirmed that all optimized structures were true minima on the potential energy surface, characterized by the absence of imaginary frequencies.

2) Structural Fragmentation and Valency Capping. Following the optimization of the full molecules, the structures were computationally fragmented to isolate the individual interacting fragments. The Cartesian coordinates of the positively charged pyridinium species and the π -system (benzene or carbazole) were extracted. To conserve appropriate chemical valency at the cleavage sites, the cut bonds were capped with H atoms. The exact geometries of these isolated, capped fragments were preserved for all subsequent evaluations.

3) Calculation of Electrostatic Potential Charges. To accurately capture the polarizing electric field generated by the pyridinium cation, single-point energy calculations were performed on the isolated pyridinium geometries using an extended basis set, ω B97X-D/def2-TZVP. Tight self-consistent field convergence criteria were applied. Partial atomic charges were derived using the CHELPG (Charges from Electrostatic Potentials using a Grid) population analysis scheme, providing an accurate representation of the external electrostatic field produced by the cation.

4) Evaluation of the Permanent and Induced Dipole Moments. The μ_{ind} of the π -system was calculated using a point-charge embedding approach to isolate the polarization effect from charge-transfer or orbital overlap interactions. First, the isolated π -system was subjected to a single-point calculation at the ω B97X-D/def2-TZVP level of theory to determine its inherent permanent dipole moment. Next, the presence of the interacting pyridinium cation was simulated by applying its previously calculated CHELPG partial charges as a background electrostatic field. Internal symmetry constraints were disabled (Symmetry=None) to preserve the exact Cartesian coordinates. The purely μ_{ind} was then obtained by vector subtraction of the isolated monomer's permanent dipole from the total electronic dipole (Pop=Dipole) generated under this perturbing point-charge field.

5) Principal Axis Alignment and Dipole Vector Transformation. To facilitate standardized visualization and subsequent comparative analyses, the final π -system and its computed quantum mechanical dipole moment were geometrically transformed to align the principal molecular plane with the Cartesian axes. First, the isolated π -system was translated such that its geometric centroid coincided with the coordinate origin (0,0,0). Singular Value Decomposition was then applied to the mean-centered atomic coordinates to extract the

Supporting Information S19

principal axes of the molecule. The atomic framework was rotated using the resulting orthogonal transformation matrix, effectively aligning the π -fragment with the xy -plane and minimizing the out-of-plane (z) atomic coordinates to near-zero. This rotation matrix was applied to the field-independent induced dipole moment vector, ensuring that the physical orientation of the dipole relative to the molecular framework was preserved in the transformed coordinate space.

Calculated geometries

1a_wB_o-1

```
Zero-point correction= 0.372280 (Hartree/Particle)
Thermal correction to Energy= 0.391941
Thermal correction to Enthalpy= 0.392885
Thermal correction to Gibbs Free Energy= 0.322522
Sum of electronic and zero-point Energies= -1033.868627
Sum of electronic and thermal Energies= -1033.848966
Sum of electronic and thermal Enthalpies= -1033.848022
Sum of electronic and thermal Free Energies= -1033.918385
```

```
E(RwB97XD) = -1034.24090678 (Hartree/Particle)
```

```
C 3.92900000 1.40500000 1.46600000
C 2.96100000 2.42200000 1.51500000
C 1.75600000 2.30900000 0.82900000
C 1.54600000 1.14500000 0.08600000
C 2.49900000 0.10400000 0.04200000
C 3.70500000 0.24500000 0.73500000
H 4.86700000 1.53200000 2.00900000
H 3.15900000 3.32300000 2.09800000
H 1.00900000 3.10400000 0.86500000
H 4.46000000 -0.54400000 0.70100000
C 0.65200000 -0.50200000 -1.18300000
C -0.18500000 -1.28300000 -1.98400000
C 0.27100000 -2.54600000 -2.35100000
C 1.52900000 -3.01700000 -1.94000000
C 2.36200000 -2.22500000 -1.15700000
C 1.92300000 -0.95500000 -0.76900000
H -1.15200000 -0.90900000 -2.32500000
H -0.35500000 -3.17400000 -2.98900000
H 1.86300000 -4.00600000 -2.25900000
H 3.34800000 -2.58600000 -0.85500000
N 0.42700000 0.76900000 -0.65900000
C -0.82300000 1.43300000 -0.63500000
C -0.98100000 2.65800000 -1.28000000
C -1.92100000 0.83900000 0.02300000
C -2.21900000 3.29900000 -1.27200000
H -0.12600000 3.09300000 -1.80000000
C -3.16800000 1.47300000 -0.01400000
C -3.31400000 2.70400000 -0.64600000
H -2.33200000 4.26100000 -1.77500000
H -4.02400000 1.01700000 0.49000000
H -4.28500000 3.20100000 -0.65000000
C -1.74800000 -0.45300000 0.71900000
C -2.60900000 -1.53100000 0.47000000
C -0.68500000 -0.67000000 1.61300000
C -2.35400000 -2.76500000 1.03000000
H -3.45600000 -1.42500000 -0.20900000
C -0.47200000 -1.92400000 2.13600000
H 0.00200000 0.13300000 1.88200000
H -2.97800000 -3.63600000 0.82900000
H 0.36400000 -2.14200000 2.80200000
N -1.28800000 -2.95700000 1.83300000
C -0.96800000 -4.30200000 2.33300000
H -0.61000000 -4.23100000 3.36600000
H -1.86900000 -4.92400000 2.30800000
H -0.19100000 -4.74800000 1.69800000
```

1a_P3_wB_o-1_e-1_A

```
E(RwB97XD) = -287.970971463 (Hartree/Particle)
```

```
C -1.74800000 -0.45300000 0.71900000
C -2.60900000 -1.53100000 0.47000000
C -0.68500000 -0.67000000 1.61300000
C -2.35400000 -2.76500000 1.03000000
H -3.45600000 -1.42500000 -0.20900000
C -0.47200000 -1.92400000 2.13600000
H 0.00200000 0.13300000 1.88200000
H -2.97800000 -3.63600000 0.82900000
H 0.36400000 -2.14200000 2.80200000
N -1.28800000 -2.95700000 1.83300000
C -0.96800000 -4.30200000 2.33300000
H -0.61000000 -4.23100000 3.36600000
H -1.86900000 -4.92400000 2.30800000
H -0.19100000 -4.74800000 1.69800000
H -1.89401710 0.49644925 0.24769847
```

1a_P3_wB_o-1_e-1_B

```
E(RwB97XD) = -517.470252379 (Hartree/Particle)
```

Supporting Information S20

```
C 3.92900000 1.40500000 1.46600000
C 2.96100000 2.42200000 1.51500000
C 1.75600000 2.30900000 0.82900000
C 1.54600000 1.14500000 0.08600000
C 2.49900000 0.10400000 0.04200000
C 3.70500000 0.24500000 0.73500000
H 4.86700000 1.53200000 2.00900000
H 3.15900000 3.32300000 2.09800000
H 1.00900000 3.10400000 0.86500000
H 4.46000000 -0.54400000 0.70100000
C 0.65200000 -0.50200000 -1.18300000
C -0.18500000 -1.28300000 -1.98400000
C 0.27100000 -2.54600000 -2.35100000
C 1.52900000 -3.01700000 -1.94000000
C 2.36200000 -2.22500000 -1.15700000
C 1.92300000 -0.95500000 -0.76900000
H -1.15200000 -0.90900000 -2.32500000
H -0.35500000 -3.17400000 -2.98900000
H 1.86300000 -4.00600000 -2.25900000
H 3.34800000 -2.58600000 -0.85500000
N 0.42700000 0.76900000 -0.65900000
H -0.39709136 1.31918197 -0.79380811
```

1b_wB_o-1

```
Zero-point correction= 0.426830 (Hartree/Particle)
Thermal correction to Energy= 0.450291
Thermal correction to Enthalpy= 0.451235
Thermal correction to Gibbs Free Energy= 0.371716
Sum of electronic and zero-point Energies= -1112.372031
Sum of electronic and thermal Energies= -1112.348570
Sum of electronic and thermal Enthalpies= -1112.347625
Sum of electronic and thermal Free Energies= -1112.427145
```

```
E(RwB97XD) = -1112.79886089 (Hartree/Particle)
```

```
C 3.96500000 1.30900000 1.38700000
C 3.03000000 2.36600000 1.37500000
C 1.83200000 2.29700000 0.67400000
C 1.56900000 1.12600000 -0.03900000
C 2.46900000 0.04200000 -0.03000000
C 3.67000000 0.14400000 0.68100000
H 3.25900000 3.27700000 1.93500000
H 1.12900000 3.13300000 0.67900000
H 4.37800000 -0.68800000 0.68100000
C 0.61700000 -0.51800000 -1.26600000
C -0.23700000 -1.29700000 -2.04800000
C 0.16600000 -2.59200000 -2.35300000
C 1.39600000 -3.12400000 -1.91100000
C 2.23800000 -2.32100000 -1.14200000
C 1.85500000 -1.01700000 -0.81300000
H -1.18400000 -0.90100000 -2.42100000
H -0.48400000 -3.21400000 -2.97400000
H 3.20200000 -2.70900000 -0.80200000
N 0.44200000 0.78100000 -0.79000000
C -0.78000000 1.49200000 -0.78600000
C -0.88600000 2.71300000 -1.44900000
C -1.90600000 0.95400000 -0.12500000
C -2.09600000 3.40300000 -1.45900000
H -0.01100000 3.10500000 -1.97000000
C -3.12700000 1.63700000 -0.18200000
C -3.21900000 2.86300000 -0.83300000
H -2.16700000 4.36200000 -1.97700000
H -4.00300000 1.22300000 0.32400000
H -4.16900000 3.39900000 -0.85200000
C -1.78900000 -0.33200000 0.59300000
C -2.69400000 -1.37700000 0.36000000
C -0.73600000 -0.57800000 1.49100000
C -2.48500000 -2.61300000 0.93300000
H -3.53700000 -1.24600000 -0.31900000
C -0.56900000 -1.83400000 2.02600000
H -0.01600000 0.20000000 1.74700000
H -3.14200000 -3.46200000 0.74200000
H 0.26100000 -2.07600000 2.69000000
N -1.42400000 -2.83800000 1.73400000
C -1.15000000 -4.18900000 2.24500000
H -0.81600000 -4.12500000 3.28600000
H -2.06400000 -4.79000000 2.19800000
H -0.36800000 -4.65500000 1.62900000
C 1.80500000 -4.51800000 -2.31500000
H 2.15900000 -4.53500000 -3.35800000
H 2.62000000 -4.90000000 -1.68500000
H 0.96200000 -5.22300000 -2.24900000
C 5.26000000 1.46100000 2.14100000
H 5.81600000 0.51400000 2.18500000
H 5.91000000 2.20700000 1.65800000
H 5.08500000 1.80100000 3.17300000
```

1b_P3_wB_o-1_e-1_A

```
E(RwB97XD) = -287.970917157 (Hartree/Particle)
```

```
C -1.78900000 -0.33200000 0.59300000
C -2.69400000 -1.37700000 0.36000000
C -0.73600000 -0.57800000 1.49100000
C -2.48500000 -2.61300000 0.93300000
H -3.53700000 -1.24600000 -0.31900000
C -0.56900000 -1.83400000 2.02600000
H -0.01600000 0.20000000 1.74700000
```

Supporting Information S21

```
H -3.14200000 -3.46200000 0.74200000
H 0.26100000 -2.07600000 2.69000000
N -1.42400000 -2.83800000 1.73400000
C -1.15000000 -4.18900000 2.24500000
H -0.81600000 -4.12500000 3.28600000
H -2.06400000 -4.79000000 2.19800000
H -0.36800000 -4.65500000 1.62900000
H -1.89559440 0.61509510 0.10663748
```

1b_P3_wB_o-1_e-1_B

E(RwB97XD) = -596.107329319 (Hartree/Particle)

```
C 3.96500000 1.30900000 1.38700000
C 3.03000000 2.36600000 1.37500000
C 1.83200000 2.29700000 0.67400000
C 1.56900000 1.12600000 -0.03900000
C 2.46900000 0.04200000 -0.03000000
C 3.67000000 0.14400000 0.68100000
H 3.25900000 3.27700000 1.93500000
H 1.12900000 3.13300000 0.67900000
H 4.37800000 -0.68800000 0.68100000
C 0.61700000 -0.51800000 -1.26600000
C -0.23700000 -1.29700000 -2.04800000
C 0.16600000 -2.59200000 -2.35300000
C 1.39600000 -3.12400000 -1.91100000
C 2.23800000 -2.32100000 -1.14200000
C 1.85500000 -1.01700000 -0.81300000
H -1.18400000 -0.90100000 -2.42100000
H -0.48400000 -3.21400000 -2.97400000
H 3.20200000 -2.70900000 -0.80200000
N 0.44200000 0.78100000 -0.79000000
C 1.80500000 -4.51800000 -2.31500000
H 2.15900000 -4.53500000 -3.35800000
H 2.62000000 -4.90000000 -1.68500000
H 0.96200000 -5.22300000 -2.24900000
C 5.26000000 1.46100000 2.14100000
H 5.81600000 0.51400000 2.18500000
H 5.91000000 2.20700000 1.65800000
H 5.08500000 1.80100000 3.17300000
H -0.35254685 1.36474853 -0.95713158
```

1c_wB_o-1

Zero-point correction= 0.597688 (Hartree/Particle)
Thermal correction to Energy= 0.628142
Thermal correction to Enthalpy= 0.629086
Thermal correction to Gibbs Free Energy= 0.536971
Sum of electronic and zero-point Energies= -1347.855818
Sum of electronic and thermal Energies= -1347.825364
Sum of electronic and thermal Enthalpies= -1347.824420
Sum of electronic and thermal Free Energies= -1347.916534

E(RwB97XD) = -1348.45350584 (Hartree/Particle)

```
C 3.94800000 1.32900000 1.43900000
C 3.03000000 2.39900000 1.46200000
C 1.82400000 2.37200000 0.76500000
C 1.52600000 1.23200000 0.02400000
C 2.42100000 0.14400000 -0.02900000
C 3.62600000 0.20300000 0.67200000
H 3.25900000 3.29300000 2.04100000
H 1.13400000 3.21800000 0.80700000
H 4.31400000 -0.64400000 0.62000000
C 0.51500000 -0.37000000 -1.19700000
C -0.38000000 -1.13000000 -1.94500000
C -0.01700000 -2.43500000 -2.26800000
C 1.21300000 -3.00200000 -1.87800000
C 2.10500000 -2.20200000 -1.15100000
C 1.76600000 -0.89300000 -0.80800000
H -1.34000000 -0.71800000 -2.26400000
H -0.72000000 -3.02400000 -2.85700000
H 3.08100000 -2.59400000 -0.85500000
N 0.36400000 0.92000000 -0.68800000
C -0.91500000 1.45900000 -0.36100000
C -1.42900000 2.56600000 -1.02700000
C -1.67000000 0.82800000 0.64900000
C -2.69500000 3.04900000 -0.69100000
H -0.83400000 3.03400000 -1.81200000
C -2.94400000 1.30100000 0.96100000
C -3.45100000 2.41600000 0.29300000
H -3.09700000 3.92000000 -1.21300000
H -3.53500000 0.80900000 1.73700000
H -4.44400000 2.79200000 0.54600000
C -1.04400000 -0.34500000 1.32100000
C -1.40700000 -1.65700000 0.98400000
C 0.02800000 -0.17100000 2.20400000
C -0.63900000 -2.71300000 1.42100000
H -2.24700000 -1.85000000 0.31700000
C 0.76800000 -1.26500000 2.60700000
H 0.34000000 0.82200000 2.52400000
H -0.84000000 -3.74500000 1.13100000
H 1.65400000 -1.16400000 3.23400000
N 0.44800000 -2.50600000 2.19600000
C 1.61800000 -4.43500000 -2.26000000
C 2.86300000 -4.38200000 -3.16400000
C 1.94400000 -5.23700000 -0.98700000
C 5.27100000 1.35800000 2.22000000
H 2.23700000 -6.26600000 -1.24100000
H 2.77900000 -4.79200000 -0.42300000
```

Supporting Information S22

```
H 1.06400000 -5.29700000 -0.32500000
H 3.72000000 -3.91500000 -2.65700000
H 3.16500000 -5.39800000 -3.46400000
C 0.50300000 -5.17200000 -3.01300000
H 2.65900000 -3.80400000 -4.07700000
H -0.41800000 -5.25000000 -2.41600000
H 0.25700000 -4.68000000 -3.96600000
H 0.82900000 -6.19600000 -3.25000000
C 5.28300000 0.19600000 3.23200000
H 5.20200000 -0.78300000 2.73400000
H 6.22100000 0.19600000 3.80800000
H 4.44900000 0.29100000 3.94600000
C 6.44700000 1.20000000 1.23800000
H 6.45000000 2.01200000 0.49600000
H 7.40500000 1.22800000 1.77900000
H 6.40400000 0.24600000 0.69100000
C 5.46100000 2.66900000 2.99200000
H 5.48800000 3.54000000 2.32000000
H 4.66600000 2.82900000 3.73700000
H 6.41800000 2.64400000 3.53400000
C 1.31400000 -3.64600000 2.52500000
H 2.05200000 -3.33800000 3.27200000
H 0.70600000 -4.46400000 2.93000000
H 1.82400000 -3.97600000 1.61100000
```

1c_P3_wB_o-1_e-1_A

E(RwB97XD) = -287.970701997 (Hartree/Particle)

```
C -1.04400000 -0.34500000 1.32100000
C -1.40700000 -1.65700000 0.98400000
C 0.02800000 -0.17100000 2.20400000
C -0.63900000 -2.71300000 1.42100000
H -2.24700000 -1.85000000 0.31700000
C 0.76800000 -1.26500000 2.60700000
H 0.34000000 0.82200000 2.52400000
H -0.84000000 -3.74500000 1.13100000
H 1.65400000 -1.16400000 3.23400000
N 0.44800000 -2.50600000 2.19600000
C 1.31400000 -3.64600000 2.52500000
H 2.05200000 -3.33800000 3.27200000
H 0.70600000 -4.46400000 2.93000000
H 1.82400000 -3.97600000 1.61100000
H -1.56904232 0.49504663 0.91658410
```

1c_P3_wB_o-1_e-1_B

E(RwB97XD) = -832.003273338 (Hartree/Particle)

```
C 3.94800000 1.32900000 1.43900000
C 3.03000000 2.39900000 1.46200000
C 1.82400000 2.37200000 0.76500000
C 1.52600000 1.23200000 0.02400000
C 2.42100000 0.14400000 -0.02900000
C 3.62600000 0.20300000 0.67200000
H 3.25900000 3.29300000 2.04100000
H 1.13400000 3.21800000 0.80700000
H 4.31400000 -0.64400000 0.62000000
C 0.51500000 -0.37000000 -1.19700000
C -0.38000000 -1.13000000 -1.94500000
C -0.01700000 -2.43500000 -2.26800000
C 1.21300000 -3.00200000 -1.87800000
C 2.10500000 -2.20200000 -1.15100000
C 1.76600000 -0.89300000 -0.80800000
H -1.34000000 -0.71800000 -2.26400000
H -0.72000000 -3.02400000 -2.85700000
H 3.08100000 -2.59400000 -0.85500000
N 0.36400000 0.92000000 -0.68800000
C 1.61800000 -4.43500000 -2.26000000
C 2.86300000 -4.38200000 -3.16400000
C 1.94400000 -5.23700000 -0.98700000
C 5.27100000 1.35800000 2.22000000
H 2.23700000 -6.26600000 -1.24100000
H 2.77900000 -4.79200000 -0.42300000
H 1.06400000 -5.29700000 -0.32500000
H 3.72000000 -3.91500000 -2.65700000
H 3.16500000 -5.39800000 -3.46400000
C 0.50300000 -5.17200000 -3.01300000
H 2.65900000 -3.80400000 -4.07700000
H -0.41800000 -5.25000000 -2.41600000
H 0.25700000 -4.68000000 -3.96600000
H 0.82900000 -6.19600000 -3.25000000
C 5.28300000 0.19600000 3.23200000
H 5.20200000 -0.78300000 2.73400000
H 6.22100000 0.19600000 3.80800000
H 4.44900000 0.29100000 3.94600000
C 6.44700000 1.20000000 1.23800000
H 6.45000000 2.01200000 0.49600000
H 7.40500000 1.22800000 1.77900000
H 6.40400000 0.24600000 0.69100000
C 5.46100000 2.66900000 2.99200000
H 5.48800000 3.54000000 2.32000000
H 4.66600000 2.82900000 3.73700000
H 6.41800000 2.64400000 3.53400000
H -0.43121026 1.51388419 -0.81023835
```

2_wB_o-1

Zero-point correction= 0.342502 (Hartree/Particle)

Supporting Information S23

Thermal correction to Energy= 0.360093
Thermal correction to Enthalpy= 0.361037
Thermal correction to Gibbs Free Energy= 0.296707
Sum of electronic and zero-point Energies= -902.450158
Sum of electronic and thermal Energies= -902.432567
Sum of electronic and thermal Enthalpies= -902.431623
Sum of electronic and thermal Free Energies= -902.495953

E(RwB97XD) = -902.792659881 (Hartree/Particle)

C	-2.17300000	2.69900000	-2.23700000
C	-2.81600000	3.31800000	-1.19800000
C	-2.44400000	3.05100000	0.14600000
C	-1.40300000	2.11100000	0.43700000
C	-0.68500000	1.54500000	-0.67600000
C	-1.09700000	1.83000000	-1.96500000
H	-3.89400000	4.45200000	0.93600000
H	-2.45900000	2.90100000	-3.27000000
C	-3.62000000	4.03200000	-1.38700000
C	-3.11100000	3.73700000	1.19800000
C	-1.14800000	1.83800000	1.83200000
H	-0.53900000	1.39900000	-2.79900000
C	-1.79900000	2.56200000	2.81800000
C	-2.77900000	3.52400000	2.50900000
H	-1.59700000	2.33700000	3.86800000
H	-3.28600000	4.06200000	3.31100000
C	0.54000000	0.70700000	-0.53200000
C	0.59300000	-0.57400000	-1.09600000
C	1.67100000	1.19400000	0.13600000
C	1.72600000	-1.37200000	-0.94800000
H	-0.27500000	-0.95700000	-1.63900000
C	2.80500000	0.39700000	0.28800000
H	1.65800000	2.20800000	0.54300000
C	2.83100000	-0.89400000	-0.24200000
H	1.75000000	-2.36900000	-1.39500000
H	3.68200000	0.79600000	0.80200000
H	3.72600000	-1.51200000	-0.14000000
C	-0.29600000	0.73300000	2.32000000
C	0.67700000	0.94800000	3.31000000
C	-0.46600000	-0.58900000	1.87100000
C	1.47600000	-0.08900000	3.73700000
H	0.85000000	1.94700000	3.71300000
C	0.36300000	-1.58600000	2.32500000
H	-1.23900000	-0.83100000	1.14300000
H	2.26800000	0.05100000	4.47300000
H	0.28500000	-2.61500000	1.97300000
C	2.25800000	-2.40600000	3.61200000
H	2.80100000	-2.11800000	4.51800000
H	1.69400000	-3.32500000	3.80800000
H	2.96900000	-2.57200000	2.79200000
N	1.33100000	-1.33200000	3.23400000

2_P3_wB_o-1_e-1_A

E(RwB97XD) = -287.970690411 (Hartree/Particle)

C	-0.29600000	0.73300000	2.32000000
C	0.67700000	0.94800000	3.31000000
C	-0.46600000	-0.58900000	1.87100000
C	1.47600000	-0.08900000	3.73700000
H	0.85000000	1.94700000	3.71300000
C	0.36300000	-1.58600000	2.32500000
H	-1.23900000	-0.83100000	1.14300000
H	2.26800000	0.05100000	4.47300000
H	0.28500000	-2.61500000	1.97300000
C	2.25800000	-2.40600000	3.61200000
H	2.80100000	-2.11800000	4.51800000
H	1.69400000	-3.32500000	3.80800000
H	2.96900000	-2.57200000	2.79200000
N	1.33100000	-1.33200000	3.23400000
H	-0.88076155	1.53767034	1.92571638

2_P3_wB_o-1_e-1_B

E(RwB97XD) = -232.245260727 (Hartree/Particle)

C	0.54000000	0.70700000	-0.53200000
C	0.59300000	-0.57400000	-1.09600000
C	1.67100000	1.19400000	0.13600000
C	1.72600000	-1.37200000	-0.94800000
H	-0.27500000	-0.95700000	-1.63900000
C	2.80500000	0.39700000	0.28800000
H	1.65800000	2.20800000	0.54300000
C	2.83100000	-0.89400000	-0.24200000
H	1.75000000	-2.36900000	-1.39500000
H	3.68200000	0.79600000	0.80200000
H	3.72600000	-1.51200000	-0.14000000
H	-0.34624779	1.30148840	-0.60977146

3_wB_o-1

Zero-point correction= 0.389757 (Hartree/Particle)
Thermal correction to Energy= 0.410285
Thermal correction to Enthalpy= 0.411229
Thermal correction to Gibbs Free Energy= 0.338609
Sum of electronic and zero-point Energies= -1055.878981
Sum of electronic and thermal Energies= -1055.858453
Sum of electronic and thermal Enthalpies= -1055.857509
Sum of electronic and thermal Free Energies= -1055.930128

Supporting Information S24

E(RwB97XD) = -1056.26873757 (Hartree/Particle)

```
C -1.91700000 3.42800000 -1.39900000
C -3.06800000 3.01900000 -0.79000000
C -3.08300000 1.82200000 -0.00500000
C -1.87300000 1.06400000 0.13000000
C -0.68300000 1.49900000 -0.55800000
C -0.72000000 2.66000000 -1.28700000
C -4.23300000 1.38000000 0.65800000
C -1.87100000 -0.07500000 0.94200000
C -3.02500000 -0.54200000 1.57400000
C -4.23700000 0.21800000 1.43900000
C -5.41100000 -0.20900000 2.13500000
H -6.32800000 0.37300000 2.01800000
C -5.39400000 -1.31400000 2.93900000
C -4.20400000 -2.07400000 3.07600000
C -3.05200000 -1.73000000 2.40200000
H -5.15300000 1.96500000 0.57600000
H -1.90600000 4.34300000 -1.99300000
H -3.98800000 3.59800000 -0.88900000
H 0.17800000 2.99200000 -1.81200000
H -0.91900000 -0.58100000 1.09100000
H -6.29500000 -1.63000000 3.46800000
H -4.22600000 -2.97800000 3.69000000
C 0.55100000 0.66500000 -0.48700000
C 0.59300000 -0.58400000 -1.12500000
C 1.67700000 1.09700000 0.22200000
C 1.73400000 -1.38100000 -1.05400000
H -0.27500000 -0.91700000 -1.70100000
C 2.81900000 0.29800000 0.29600000
H 1.65500000 2.06800000 0.72100000
C 2.85000000 -0.94300000 -0.33800000
H 1.76400000 -2.33500000 -1.58700000
H 3.69300000 0.65300000 0.84700000
H 3.75200000 -1.55700000 -0.29500000
C -1.87500000 -2.60600000 2.51000000
C -1.45100000 -3.11300000 3.75300000
C -1.12100000 -2.99300000 1.38200000
C -0.33200000 -3.91200000 3.83800000
H -1.97800000 -2.84800000 4.67000000
C -0.01000000 -3.78900000 1.52500000
H -1.40600000 -2.67100000 0.38100000
H 0.03300000 -4.29900000 4.79000000
H 0.60200000 -4.09200000 0.67400000
C 1.60300000 -5.04800000 2.84400000
H 1.72600000 -5.38800000 3.87700000
H 1.51900000 -5.92000000 2.18400000
H 2.47100000 -4.44200000 2.55400000
N 0.38300000 -4.23400000 2.74000000
```

3_P3_wB_o-1_e-1_A

E(RwB97XD) = -287.970618658 (Hartree/Particle)

```
C -1.87500000 -2.60600000 2.51000000
C -1.45100000 -3.11300000 3.75300000
C -1.12100000 -2.99300000 1.38200000
C -0.33200000 -3.91200000 3.83800000
H -1.97800000 -2.84800000 4.67000000
C -0.01000000 -3.78900000 1.52500000
H -1.40600000 -2.67100000 0.38100000
H 0.03300000 -4.29900000 4.79000000
H 0.60200000 -4.09200000 0.67400000
C 1.60300000 -5.04800000 2.84400000
H 1.72600000 -5.38800000 3.87700000
H 1.51900000 -5.92000000 2.18400000
H 2.47100000 -4.44200000 2.55400000
N 0.38300000 -4.23400000 2.74000000
H -2.72451284 -1.96099750 2.42514887
```

3_P3_wB_o-1_e-1_B

E(RwB97XD) = -232.245417453 (Hartree/Particle)

```
C 0.55100000 0.66500000 -0.48700000
C 0.59300000 -0.58400000 -1.12500000
C 1.67700000 1.09700000 0.22200000
C 1.73400000 -1.38100000 -1.05400000
H -0.27500000 -0.91700000 -1.70100000
C 2.81900000 0.29800000 0.29600000
H 1.65500000 2.06800000 0.72100000
C 2.85000000 -0.94300000 -0.33800000
H 1.76400000 -2.33500000 -1.58700000
H 3.69300000 0.65300000 0.84700000
H 3.75200000 -1.55700000 -0.29500000
H -0.32591223 1.27567978 -0.54172788
```

For compounds **1a**, **1b**, **1c**, **2**, and **3** the μ_{ind} towards the cation is given in Table S3.

Table S3. The calculated μ_{ind} values for **1b**, **1c**, **2**, and **3**.

Compound	μ_{ind}, D	$\frac{\mu_{\text{ge}}}{M^{-0.5} \times \text{cm}^{-0.5}}$
1a	0.95	26.38
1b	1.15	26.83
1c	1.43	27.42
2	0.82	81.67
3	0.68	80.54

Since $\varepsilon \propto |\mu_{\text{ge}}|^2$, then $\mu_{\text{ge}} \propto \sqrt{\varepsilon}$, the calculated values of μ_{ge} , is given in Table S3.

We find that $\lg(n_4) \propto \mu_{\text{ge}} \times \mu_{\text{ind}}$ (see Figure S9), confirming that the fifth-order nonlinear refractive response is governed by the electric-field-induced polarization of the π -system towards the cation.

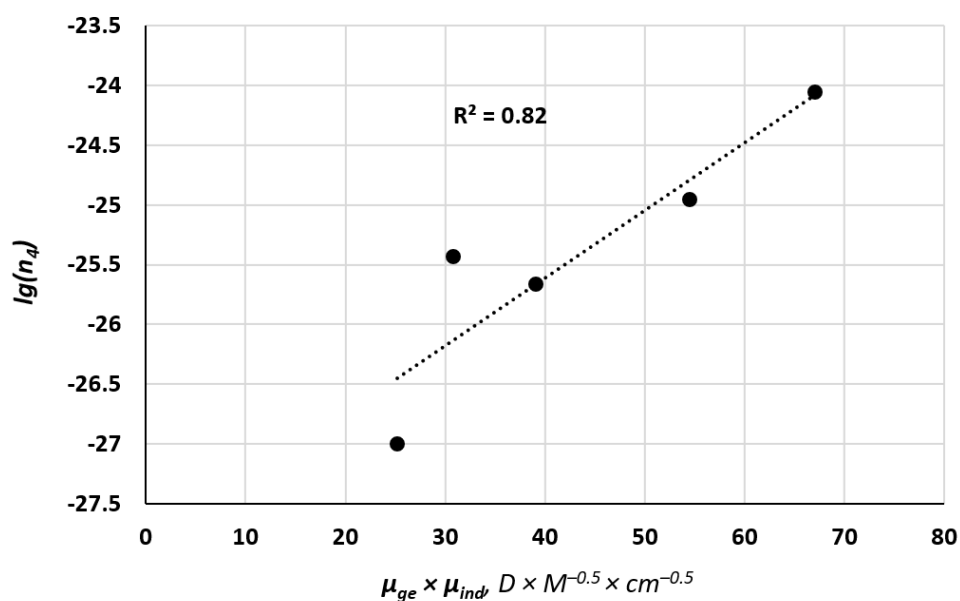


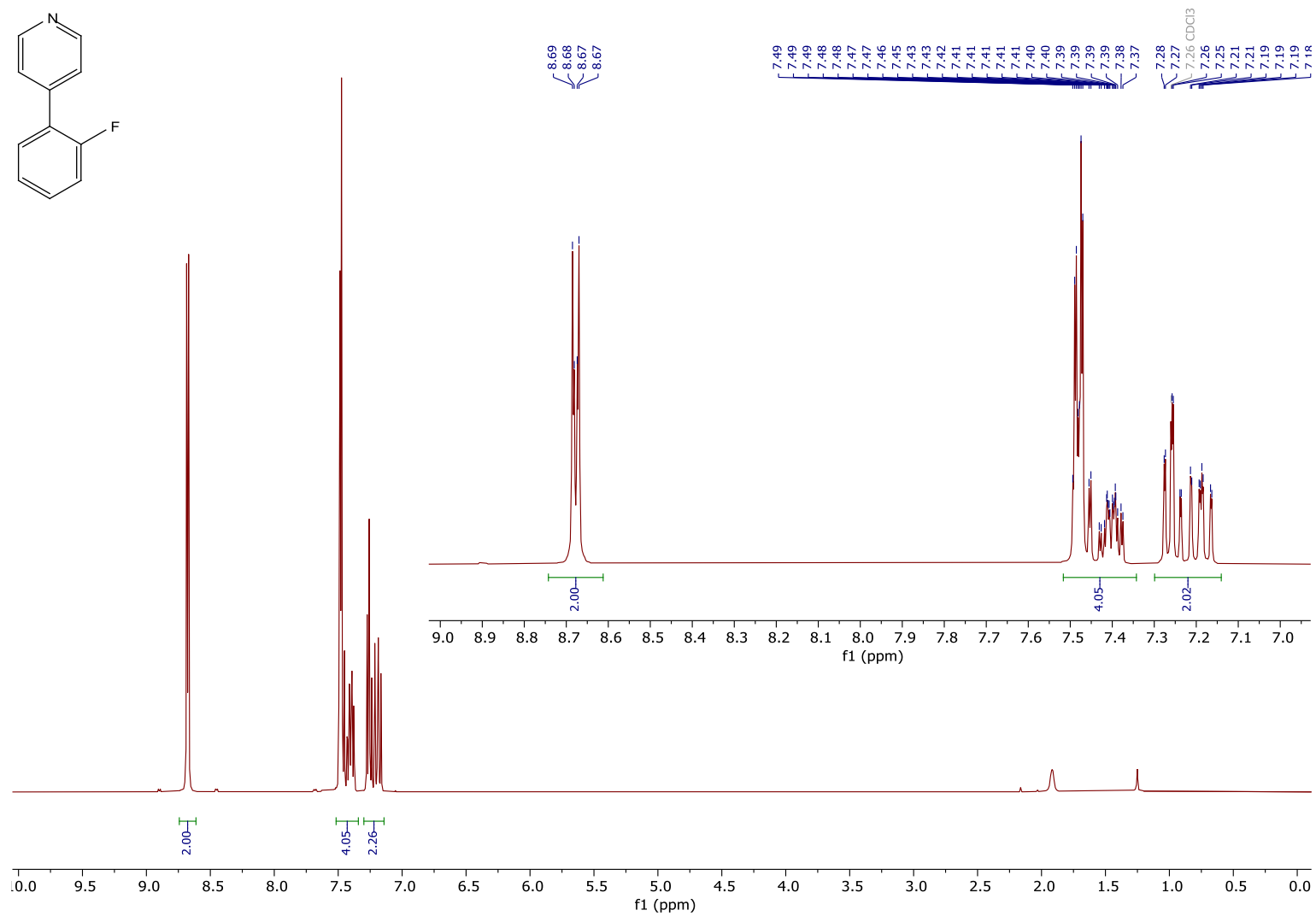
Fig. S9. $\lg(n_4)$ relation to $\mu_{\text{ge}} \times \mu_{\text{ind}}$.

References:

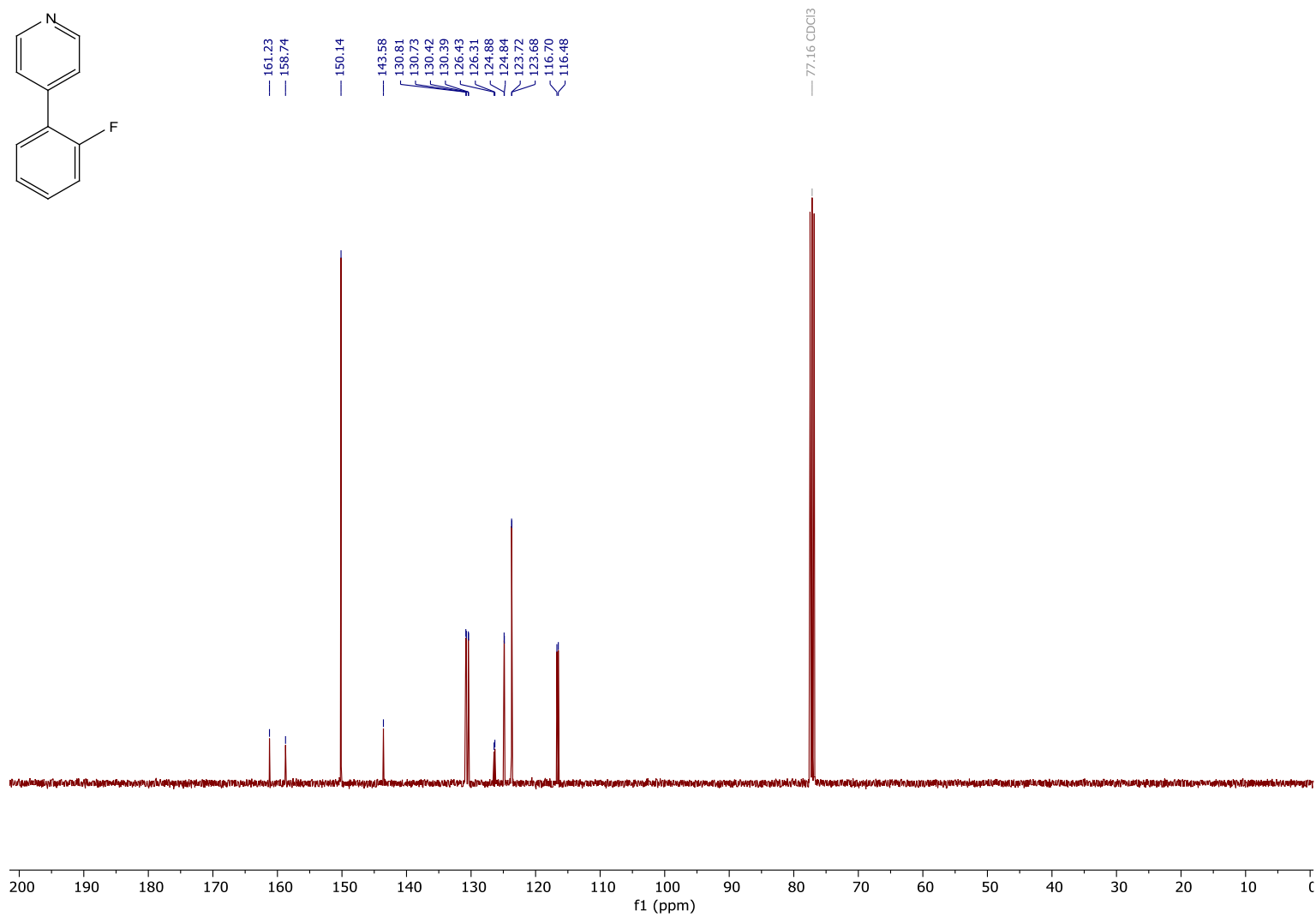
- 1) A. A. Bartolomeu, R. C. Silva, T. J. Brocksom, T. Noël, K. T. Oliveira. *J. Org. Chem.* **2019**, *84*, 10459–10471.
- 2) K. Leduskrasts, A. Kinens, E. Suna. *Chem. Commun.* **2019**, *55*, 12663–12666.
- 3) M. Sheik-Bahae, A. A. Said, T.-H. Wei, D. J. Hagan and E. W. Van Stryland. *IEEE Journal of Quantum Electronics*, **1990**, *26*, 760–769.

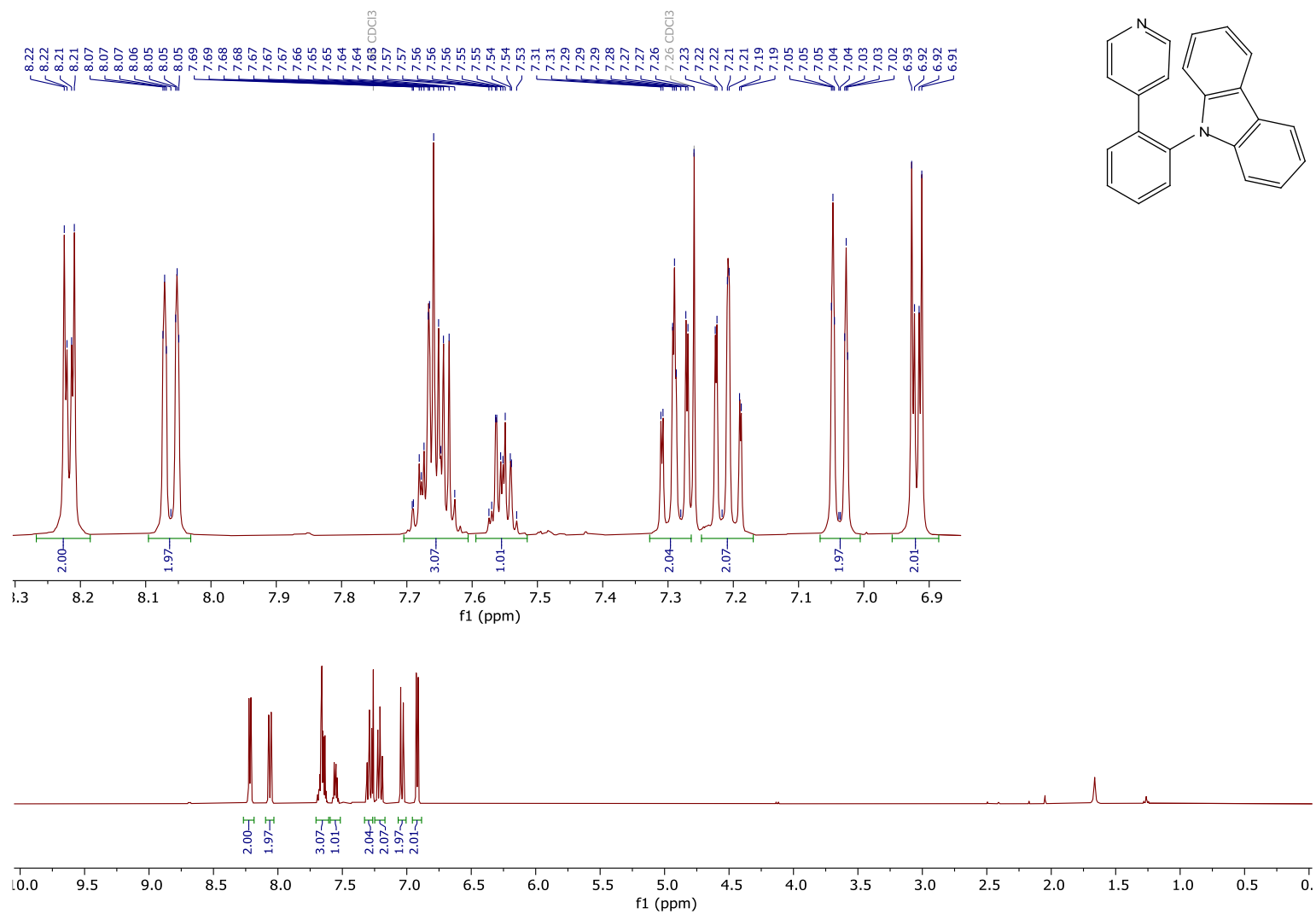
- 4) Yan, X.-Q., Liu, Z.-B., Zhang, X.-L., Zhou, W.-Y., & Tian, J.-G. *Optics Express*, **2009**, 17(8), 6397.
- 5) Yan, X.-Q.; Zhang, X.-L.; Shi, S.; Liu, Z.-B.; Tian, J.-G. *Optics Express* **2011**, 19 (6), 5559.
- 6) Moysés, R. M.; Barbano, E. C.; Misoguti, L. *Journal of the Optical Society of America B* **2023**, 40 (4), C60–C66.
- 7) Miguez, M. L.; De Souza, T. G.; Barbano, E. C.; Zilio, S. C.; Misoguti, L. *Optics Express* **2017**, 25 (4), 3553.
- 8) Bundulis, A.; Mihailovs, I.; Rutkis, M. *Journal of the Optical Society of America B* **2020**, 37 (6), 1806.
- 9) Melhado, M. S.; de Souza, T. G.; Zilio, S. C.; Barbano, E. C.; Misoguti, L. *Optics Express* **2020**, 28 (3), 3352.
- 10) Méndez Rodríguez, J. J.; García Ramírez, E. V.; Arroyo Carrasco, M. L.; Méndez Otero, M. M.; Torres Romero, R.; Martínez Irvias, B. A.; Iturbe Castillo, M. D. *Journal of the Optical Society of America B* **2025**, 43 (1), 120.

^1H and ^{13}C NMR data

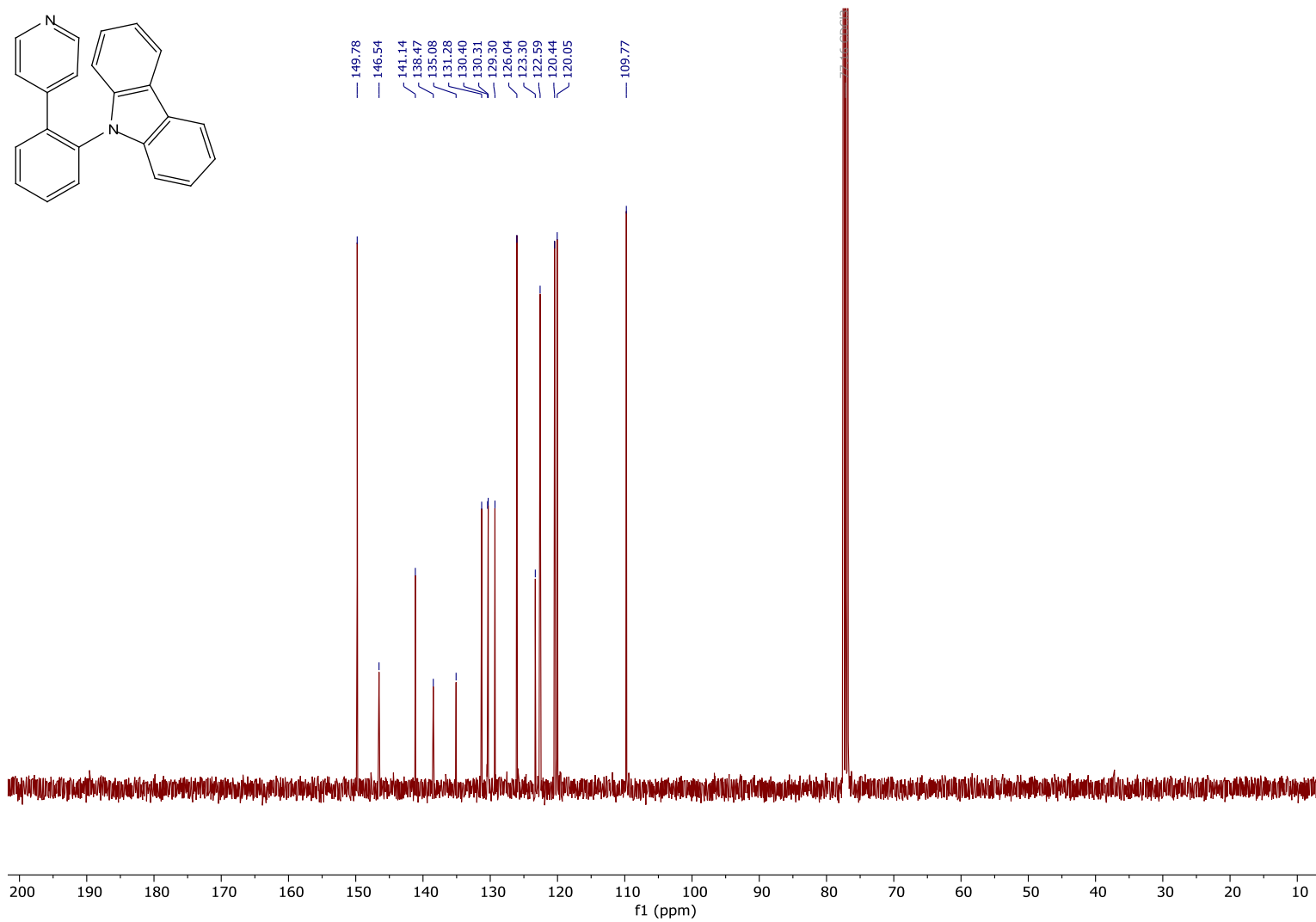
^1H NMR (400 MHz, CDCl_3 , ppm) spectrum of 4-(2-Fluorophenyl)pyridine (**8**).

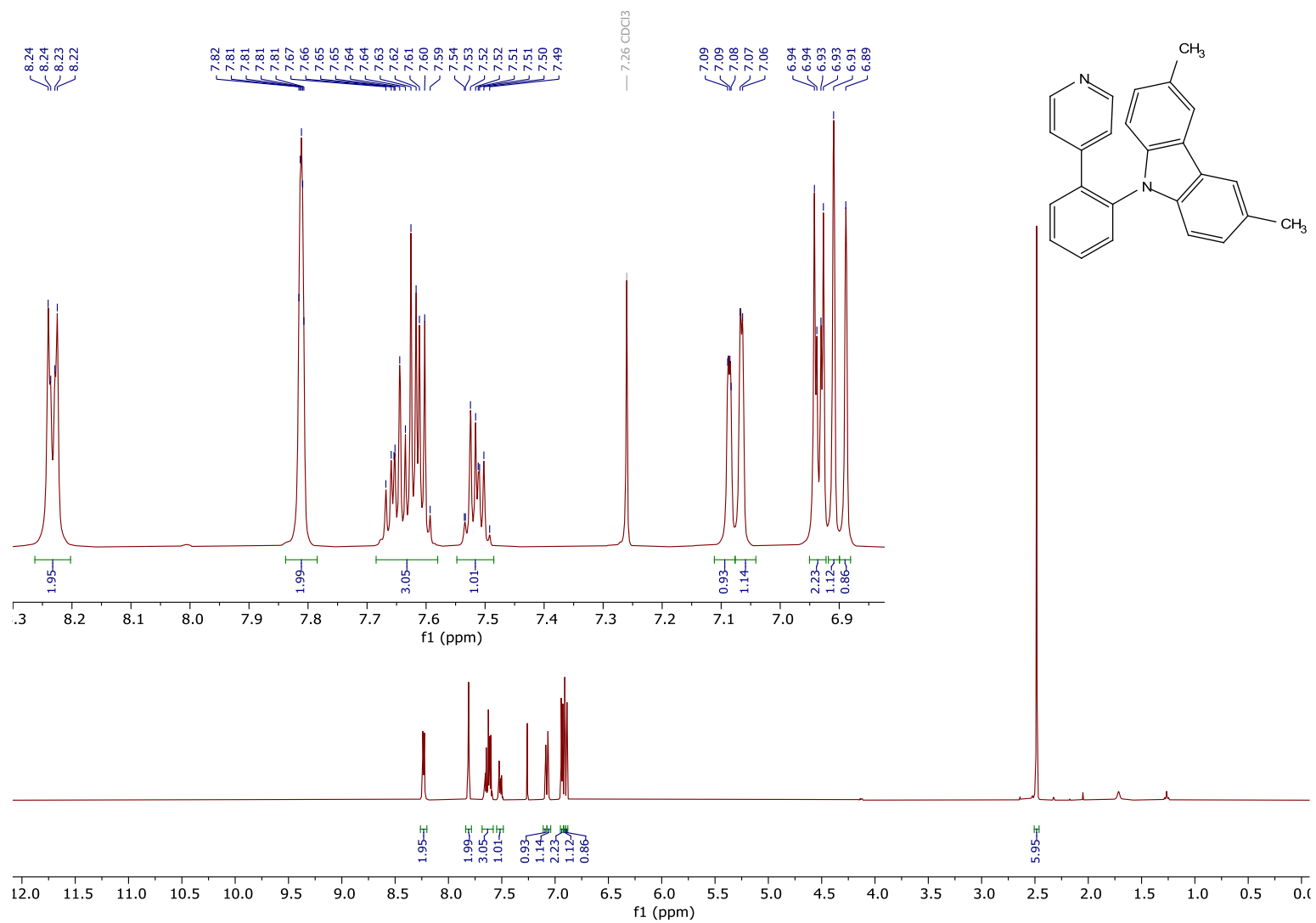
$^{13}\text{C}\{^1\text{H}\}$ NMR (101 MHz, CDCl_3 , ppm) spectrum of 4-(2-Fluorophenyl)pyridine (**8**).



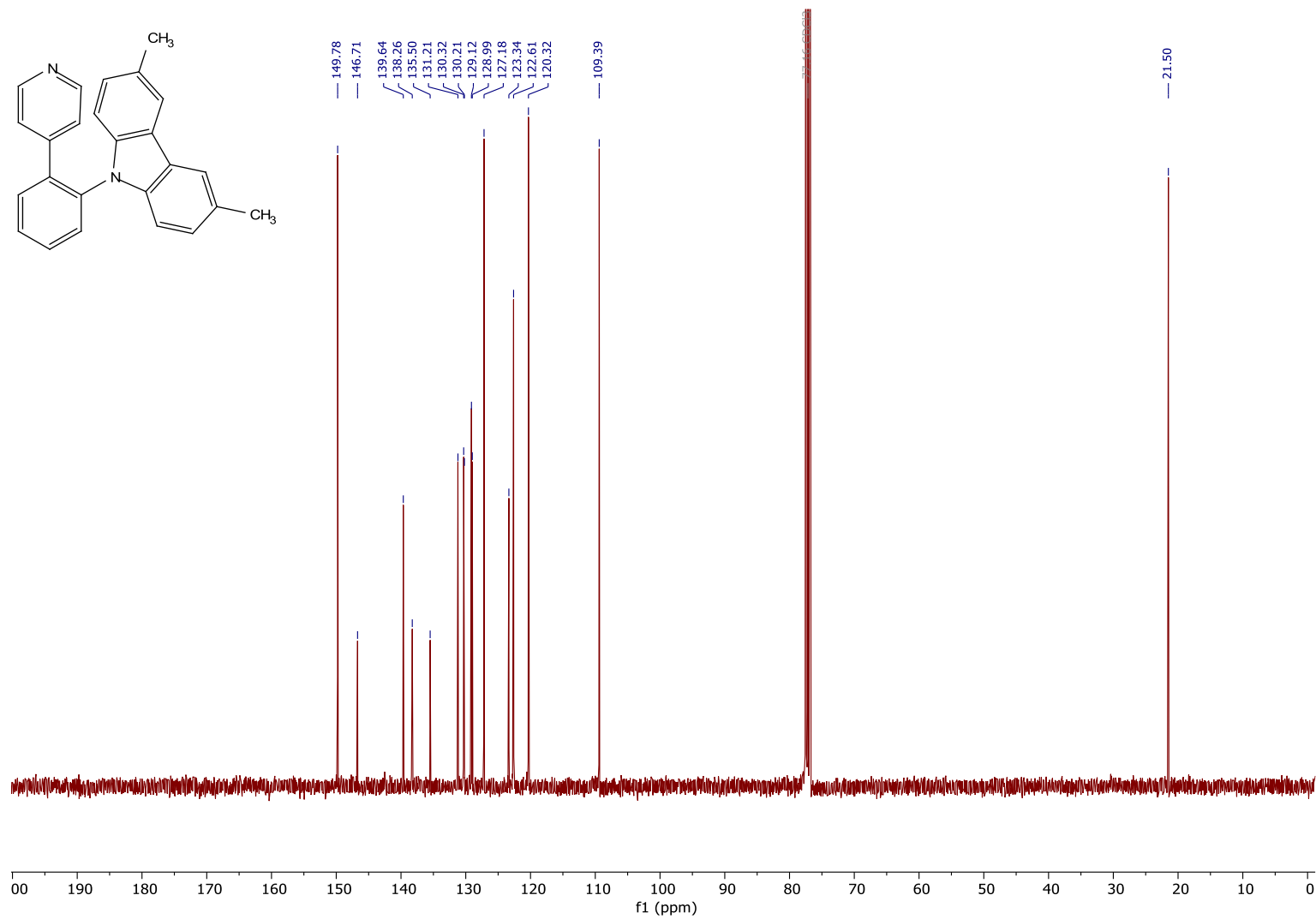
^1H NMR (400 MHz, CDCl_3 , ppm) spectrum of 9-(2-(pyridin-4-yl)phenyl)-9H-carbazole (**5a**)

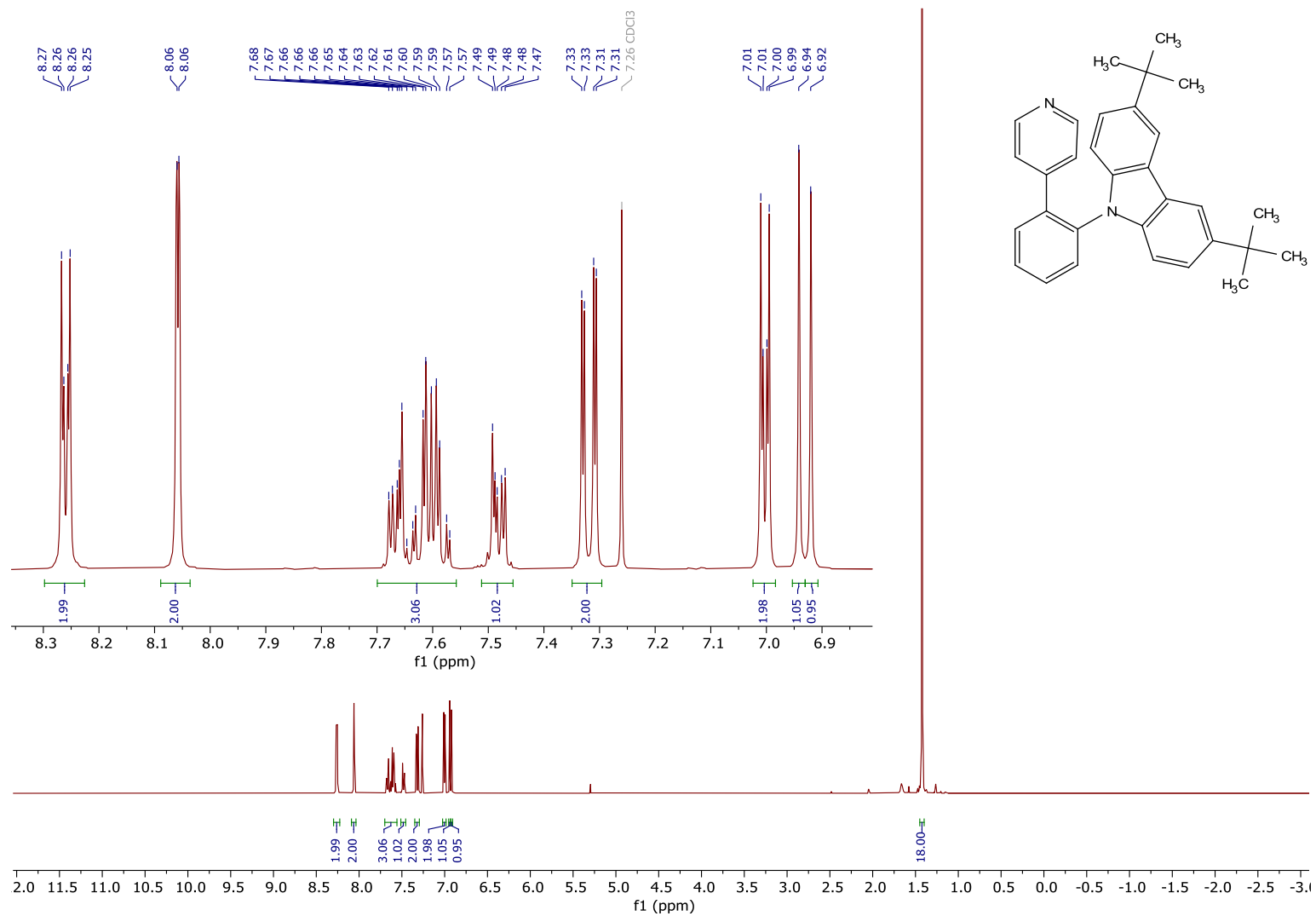
$^{13}\text{C}\{^1\text{H}\}$ NMR (101 MHz, CDCl_3 , ppm) spectrum of 9-(2-(pyridin-4-yl)phenyl)-9H-carbazole (**5a**)



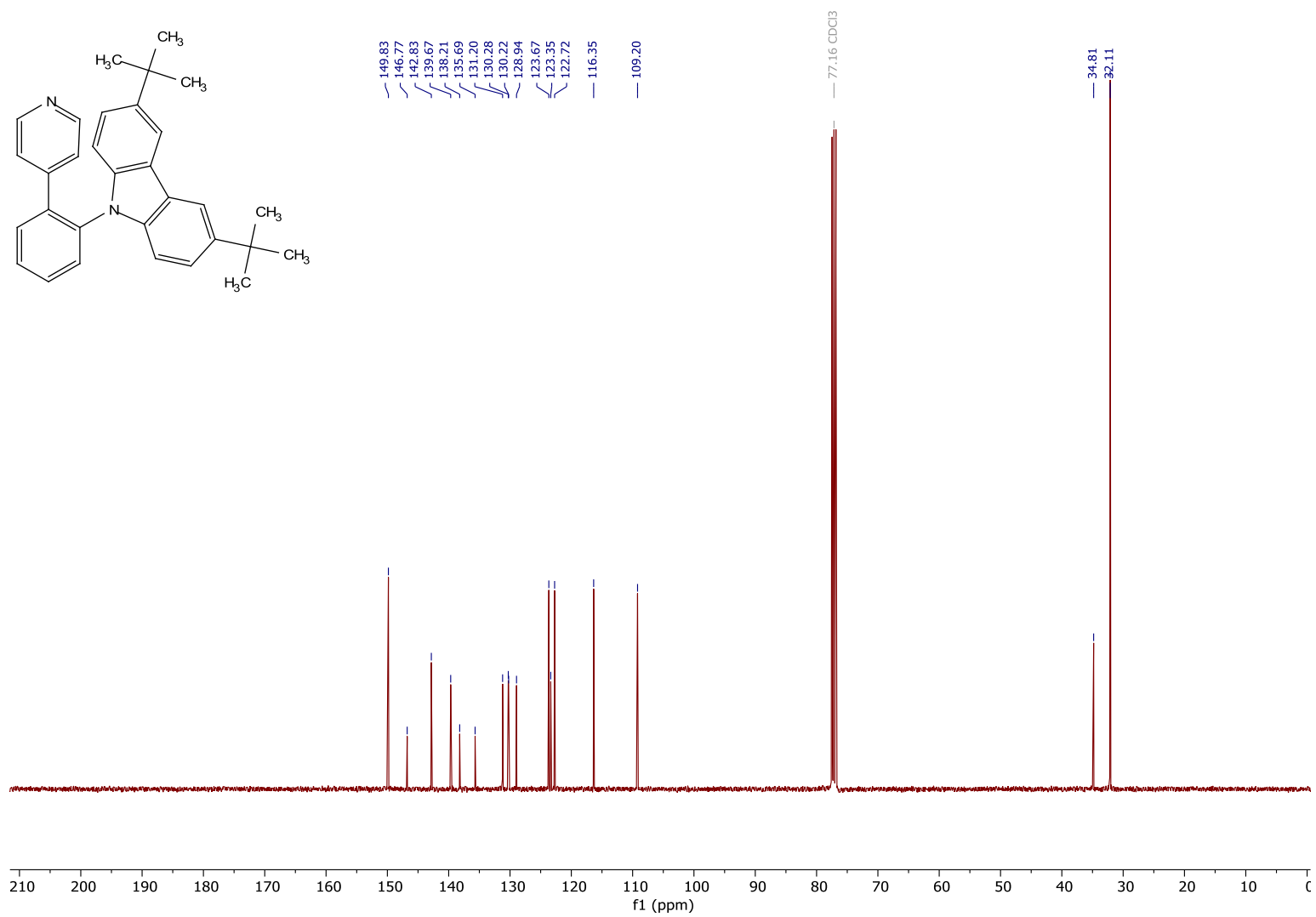
^1H NMR (400 MHz, CDCl_3 , ppm) spectrum of 3,6-dimethyl-9-(2-(pyridin-4-yl)phenyl)-9H-carbazole **5b**

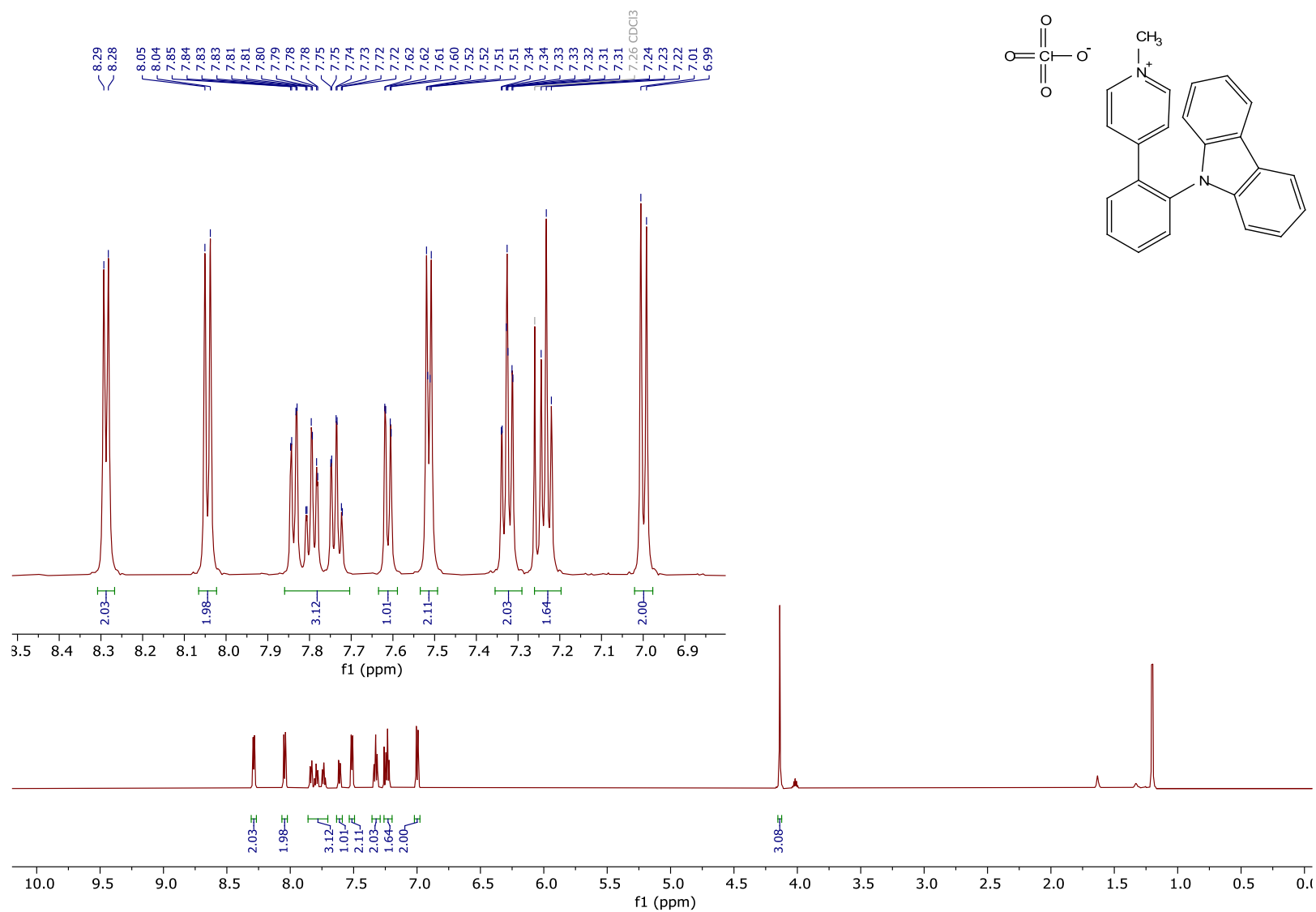
$^{13}\text{C}\{^1\text{H}\}$ NMR (101 MHz, CDCl_3 , ppm) spectrum of 3,6-dimethyl-9-(2-(pyridin-4-yl)phenyl)-9H-carbazole **5b**



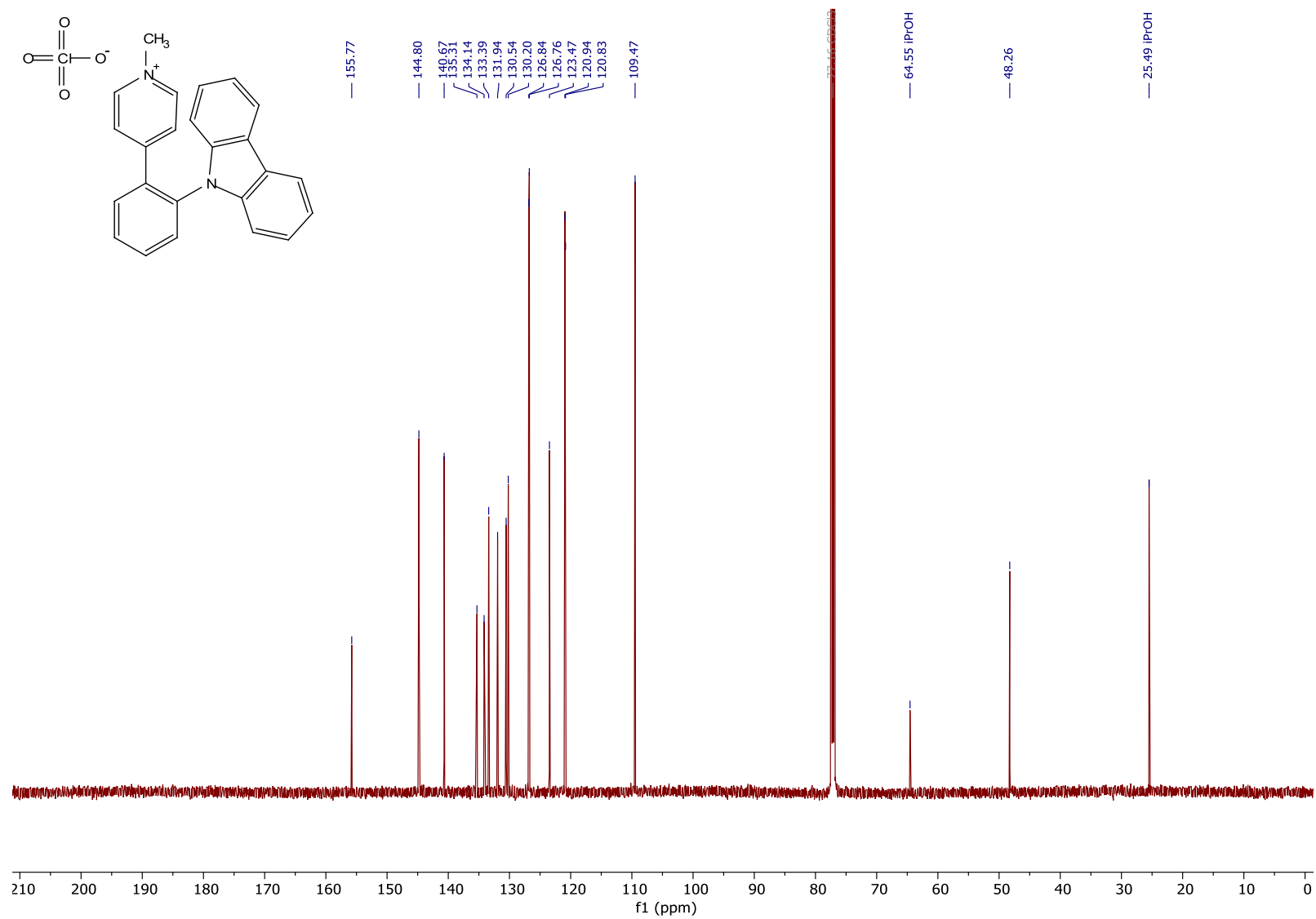
^1H NMR (400 MHz, CDCl_3 , ppm) spectrum of 3,6-di-*tert*-butyl-9-(2-(pyridin-4-yl)phenyl)-9*H*-carbazole (**5c**)

$^{13}\text{C}\{^1\text{H}\}$ NMR (101 MHz, CDCl_3 , ppm) spectrum of 3,6-di-*tert*-butyl-9-(2-(pyridin-4-yl)phenyl)-9*H*-carbazole (**5c**)

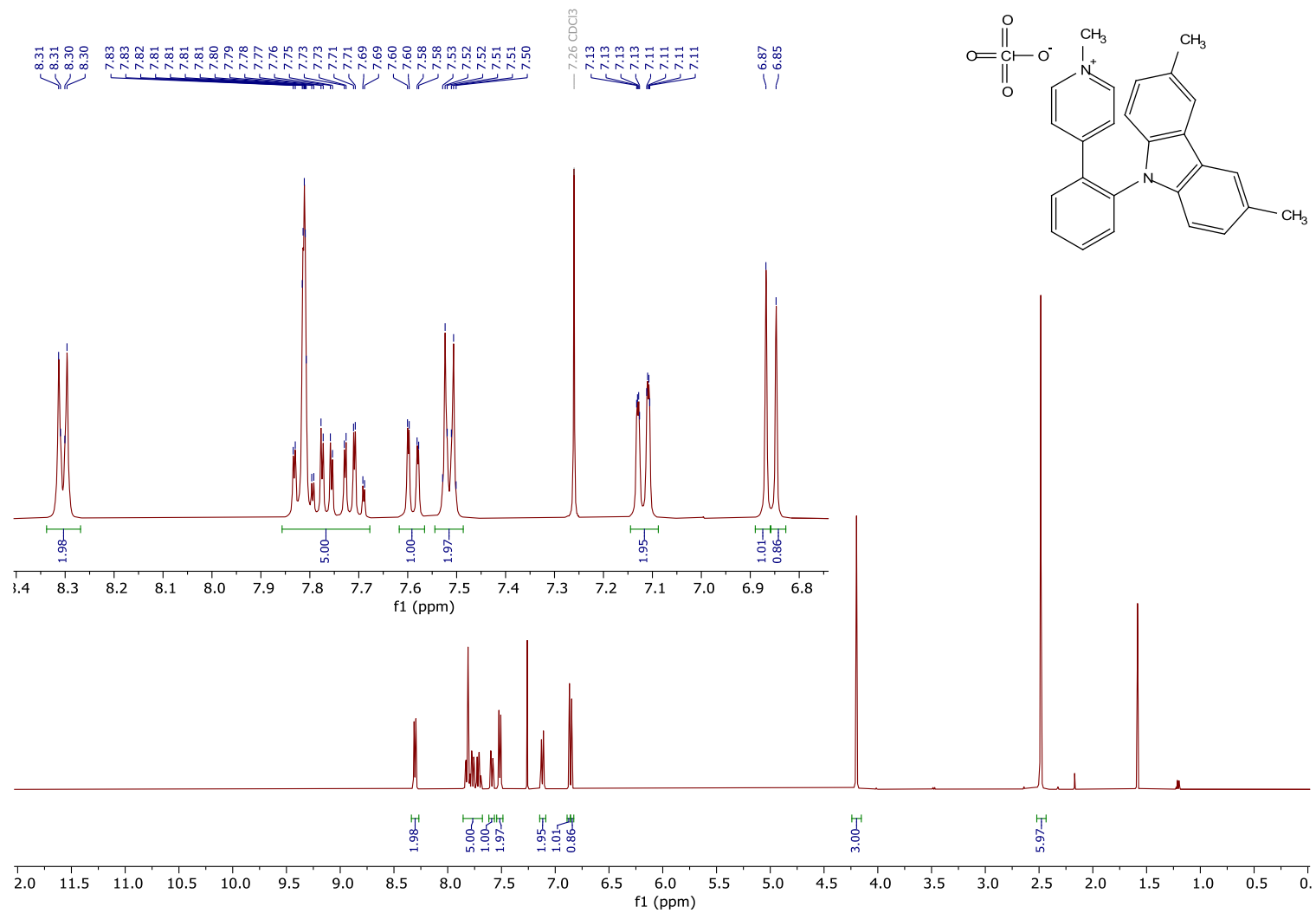


^1H NMR (400 MHz, CDCl_3 , ppm) spectrum of 4-(2-(9*H*-carbazol-9-yl)phenyl)-1-methylpyridin-1-ium perchlorate (**1a**)

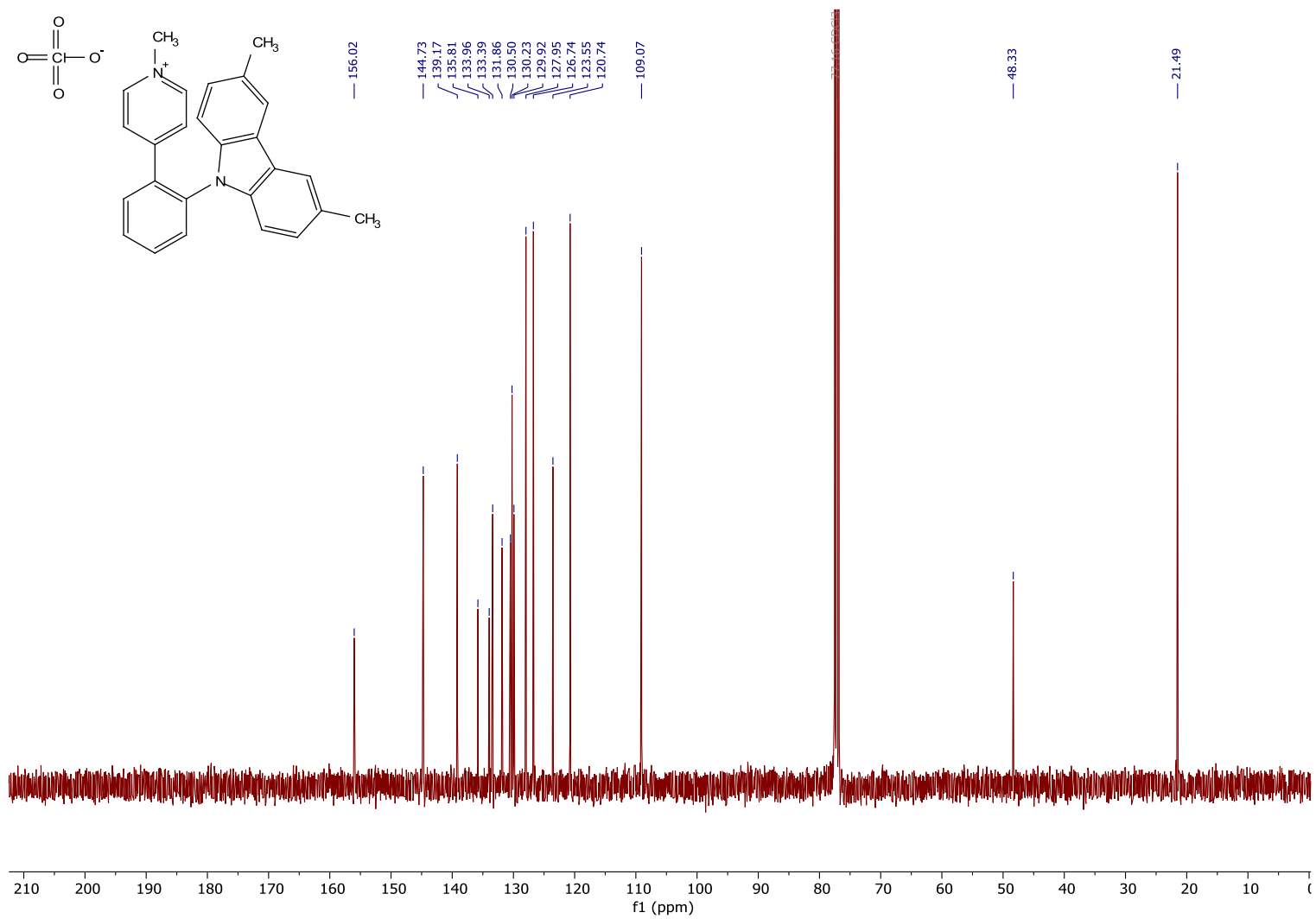
$^{13}\text{C}\{^1\text{H}\}$ NMR (101 MHz, CDCl_3 , ppm) spectrum of 4-(2-(9*H*-carbazol-9-yl)phenyl)-1-methylpyridin-1-ium perchlorate (**1a**)



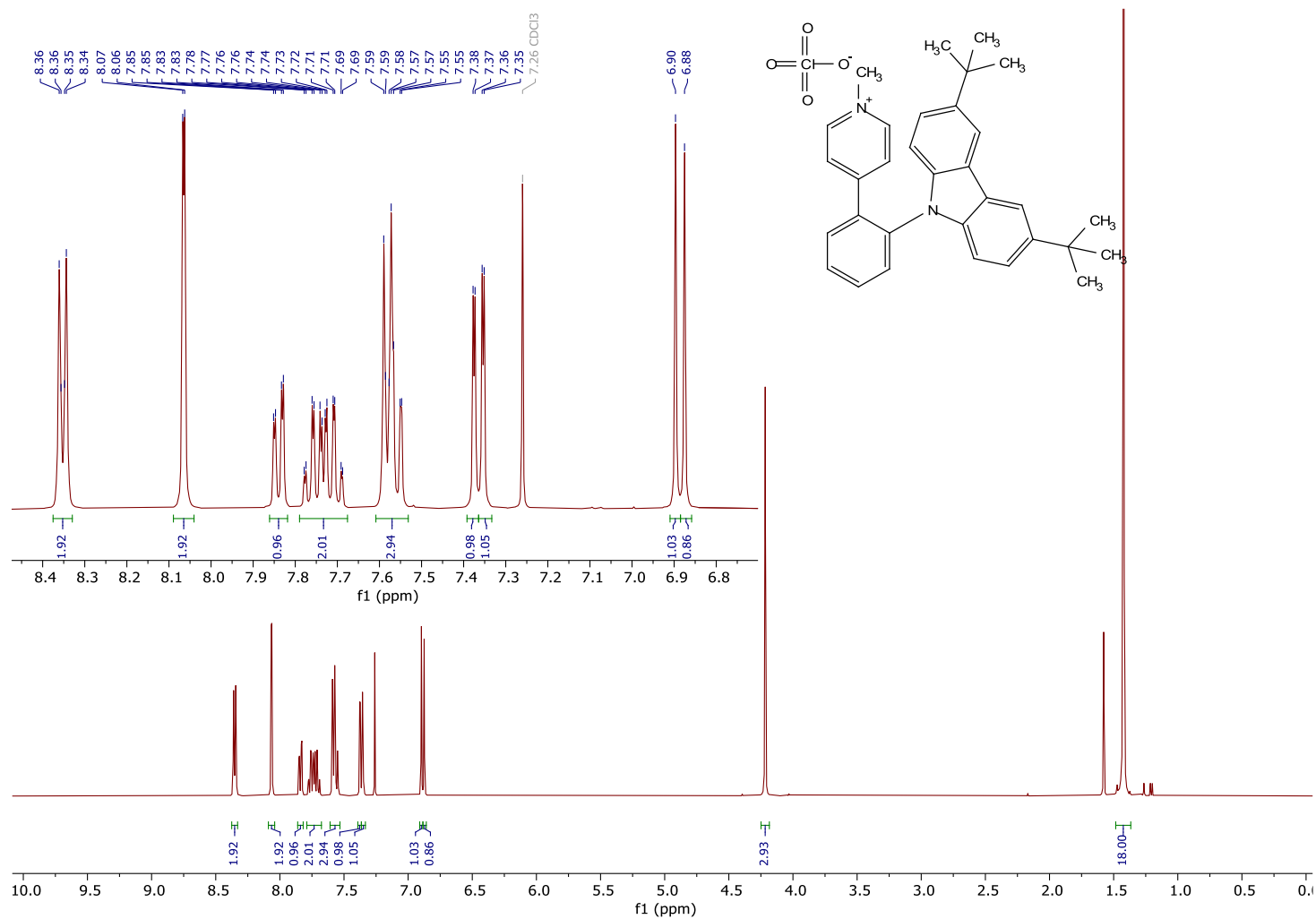
^1H NMR (400 MHz, CDCl_3 , ppm) spectrum of 4-(2-(3,6-dimethyl-9H-carbazol-9-yl)phenyl)-1-methylpyridin-1-ium perchlorate (**1b**)



$^{13}\text{C}\{^1\text{H}\}$ NMR (101 MHz, CDCl_3 , ppm) spectrum of 4-(2-(3,6-dimethyl-9H-carbazol-9-yl)phenyl)-1-methylpyridin-1-ium perchlorate (**1b**)

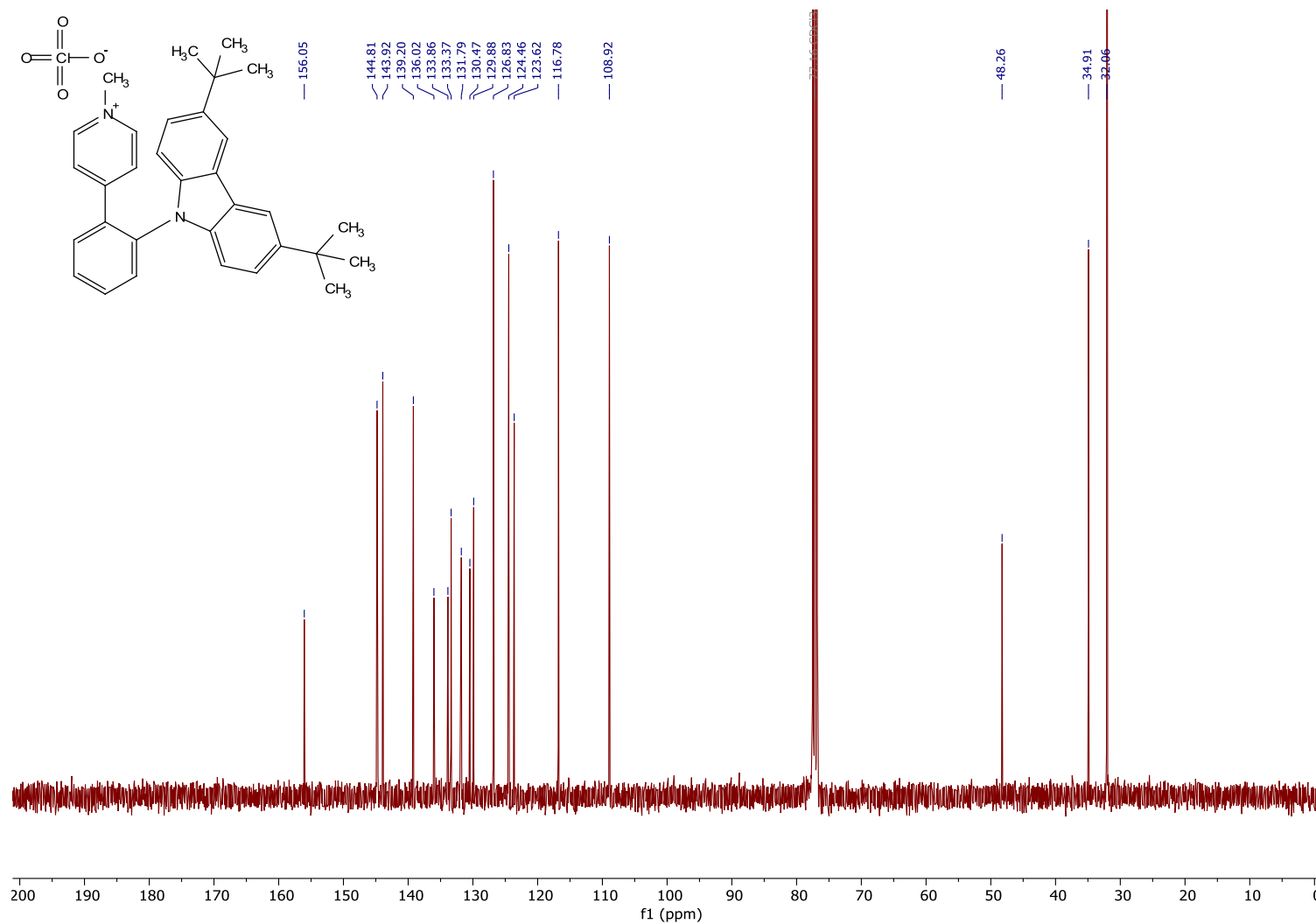


^1H NMR (400 MHz, CDCl_3 , ppm) spectrum of 4-(2-(3,6-di-*tert*-butyl-9*H*-carbazol-9-yl)phenyl)-1-methylpyridin-1-ium perchlorate (**1c**)



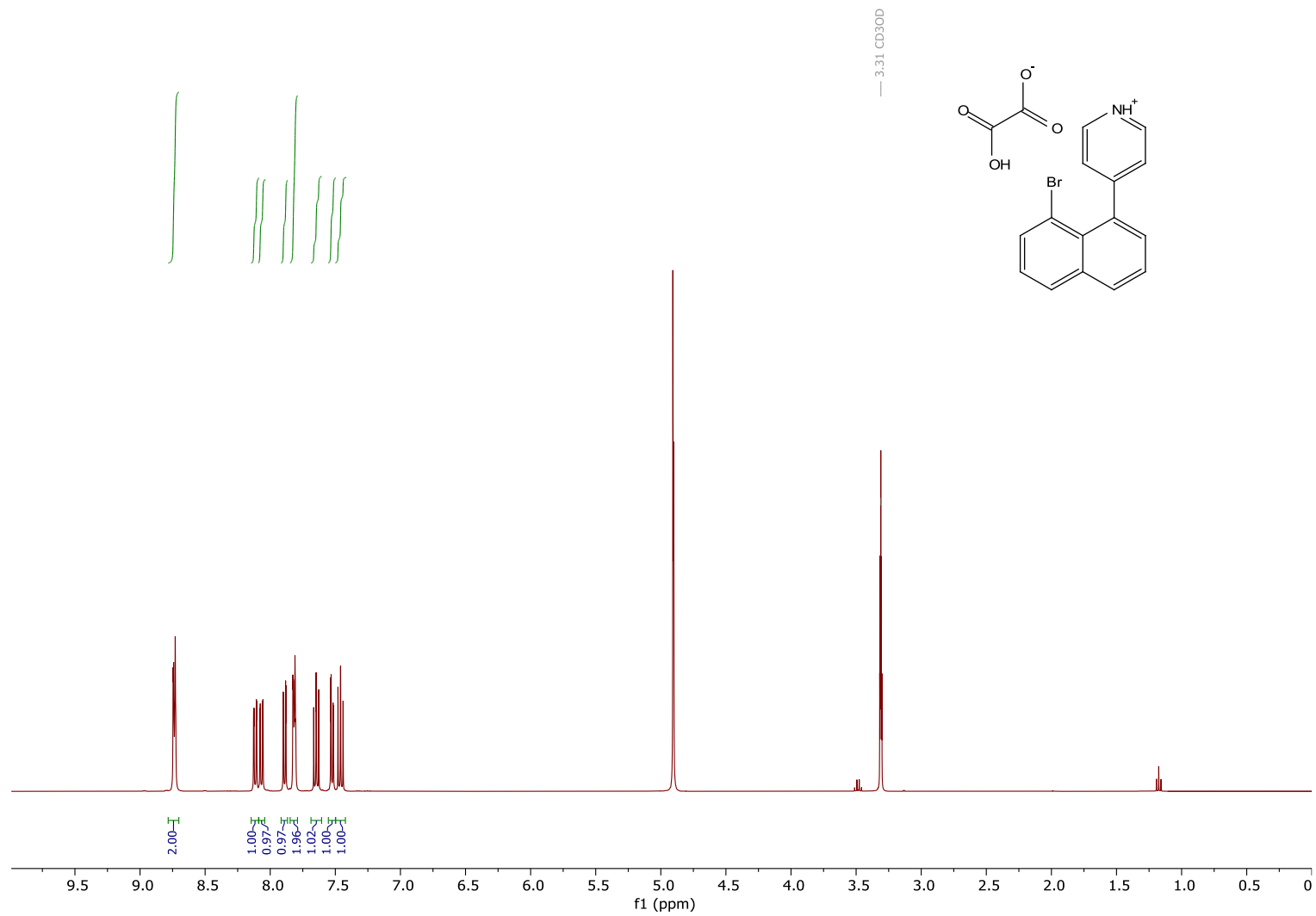
Supporting Information S41

$^{13}\text{C}\{^1\text{H}\}$ NMR (101 MHz, CDCl_3 , ppm) spectrum of 4-(2-(3,6-di-*tert*-butyl-9*H*-carbazol-9-yl)phenyl)-1-methylpyridin-1-ium perchlorate (**1c**)



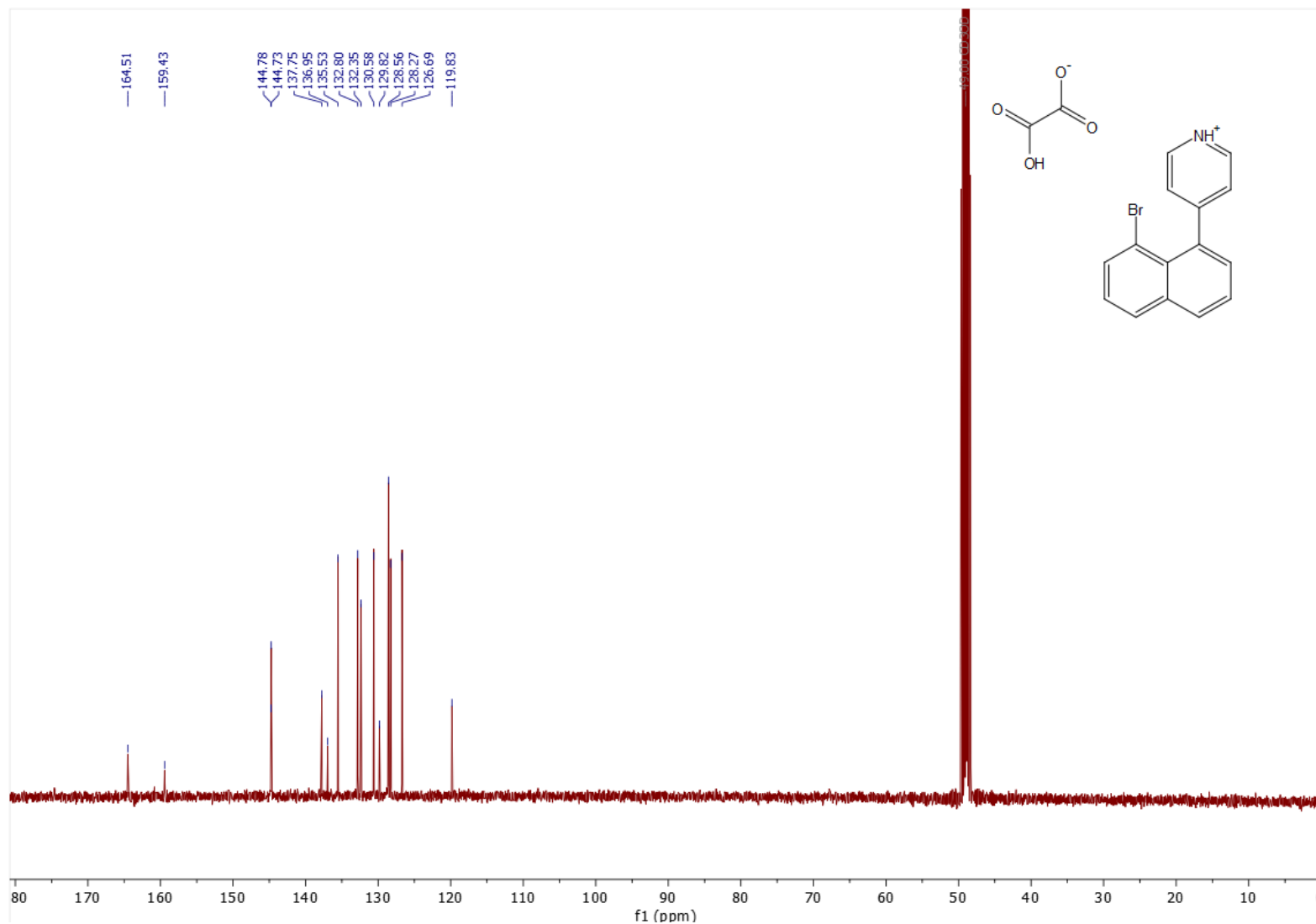
Supporting Information S42

^1H NMR (400 MHz, CD_3OD , ppm) spectrum of 4-(8-Bromonaphthalen-1-yl)pyridin-1-ium carboxyformate (**11**)



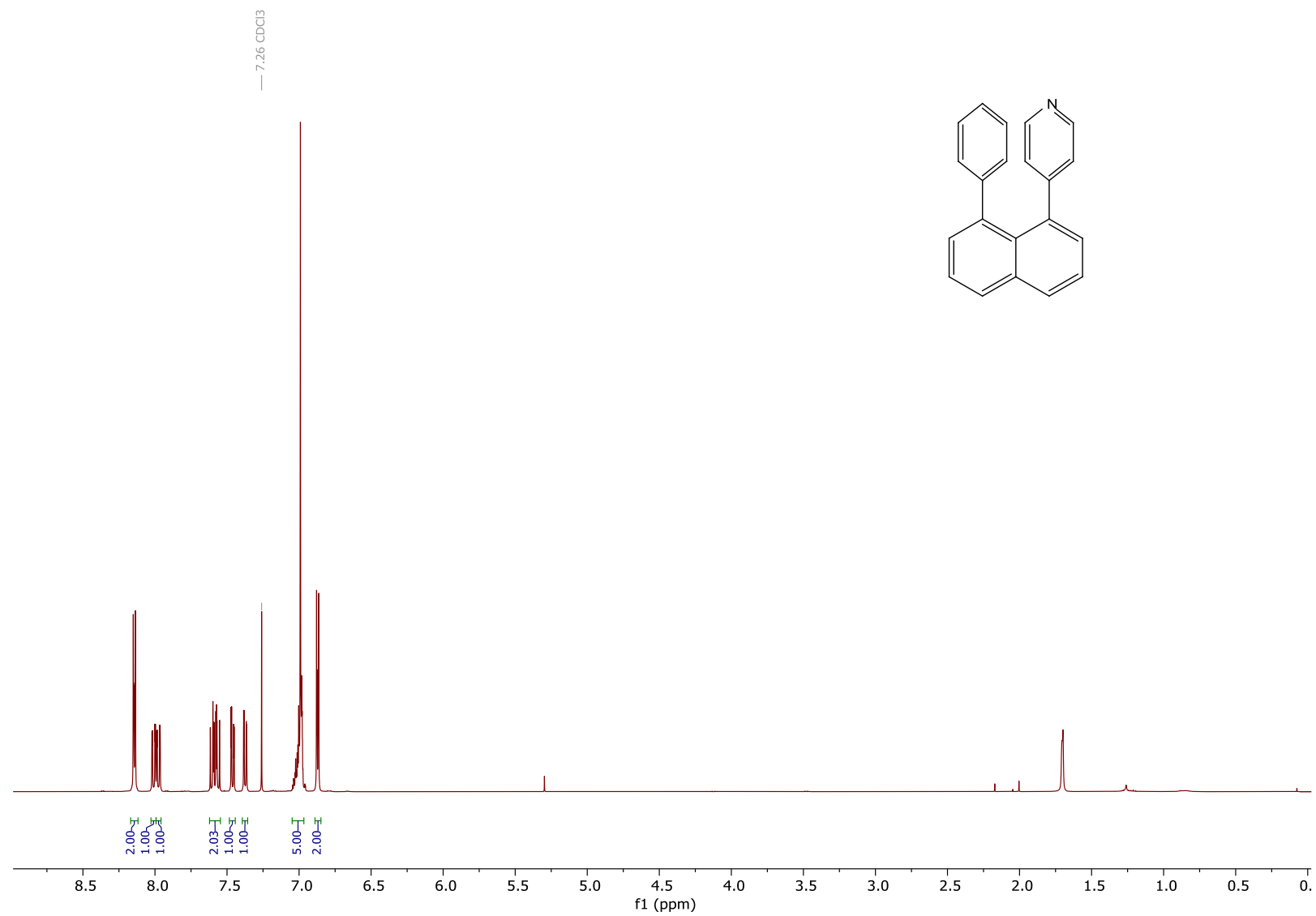
Supporting Information S43

$^{13}\text{C}\{^1\text{H}\}$ NMR (101 MHz, CD_3OD , ppm) spectrum of 4-(8-Bromonaphthalen-1-yl)pyridin-1-ium carboxyformate (**11**)



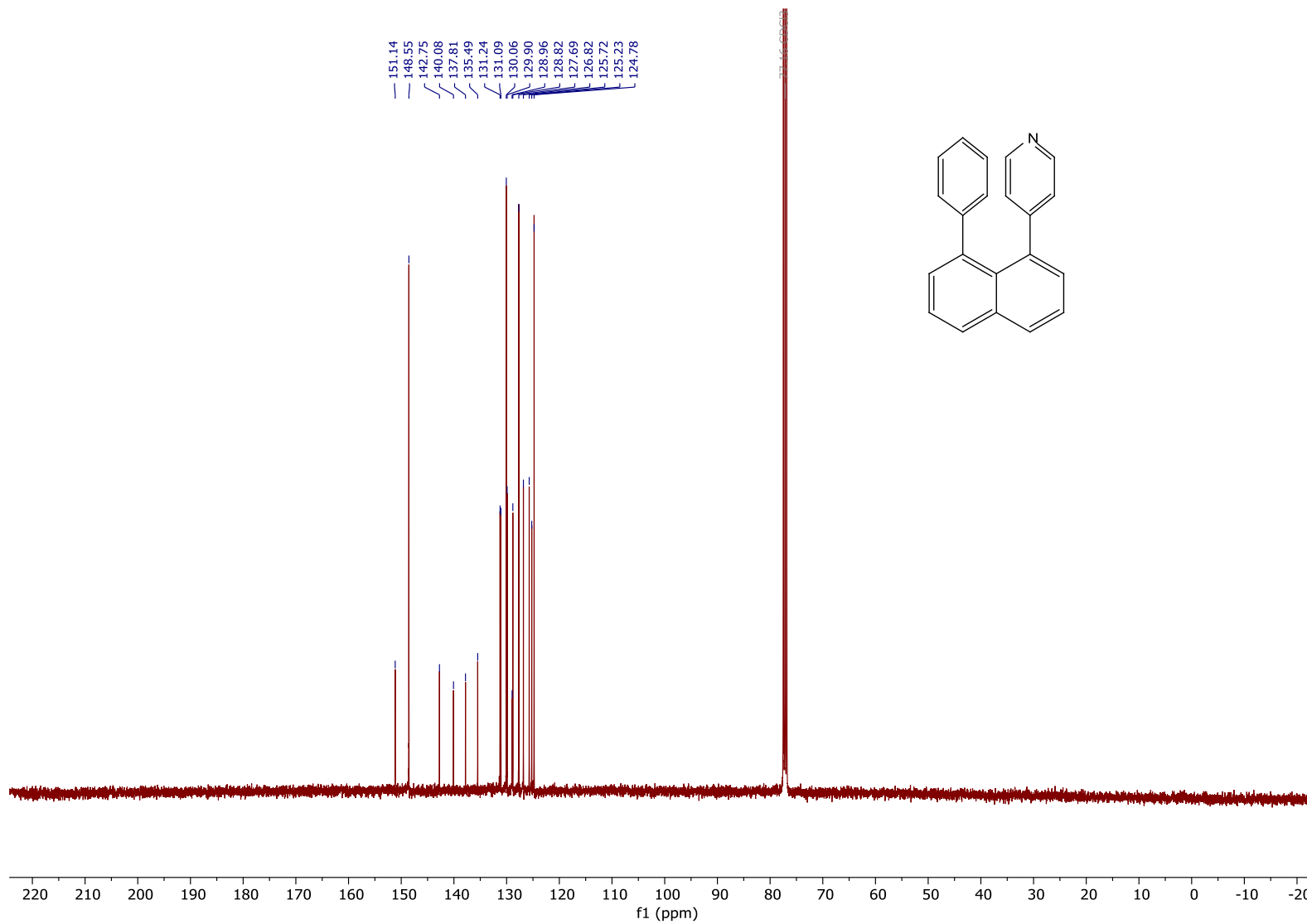
Supporting Information S44

^1H NMR (400 MHz, CDCl_3 , ppm) spectrum of 4-(8-Phenyl-naphthalen-1-yl)pyridine (**12**)



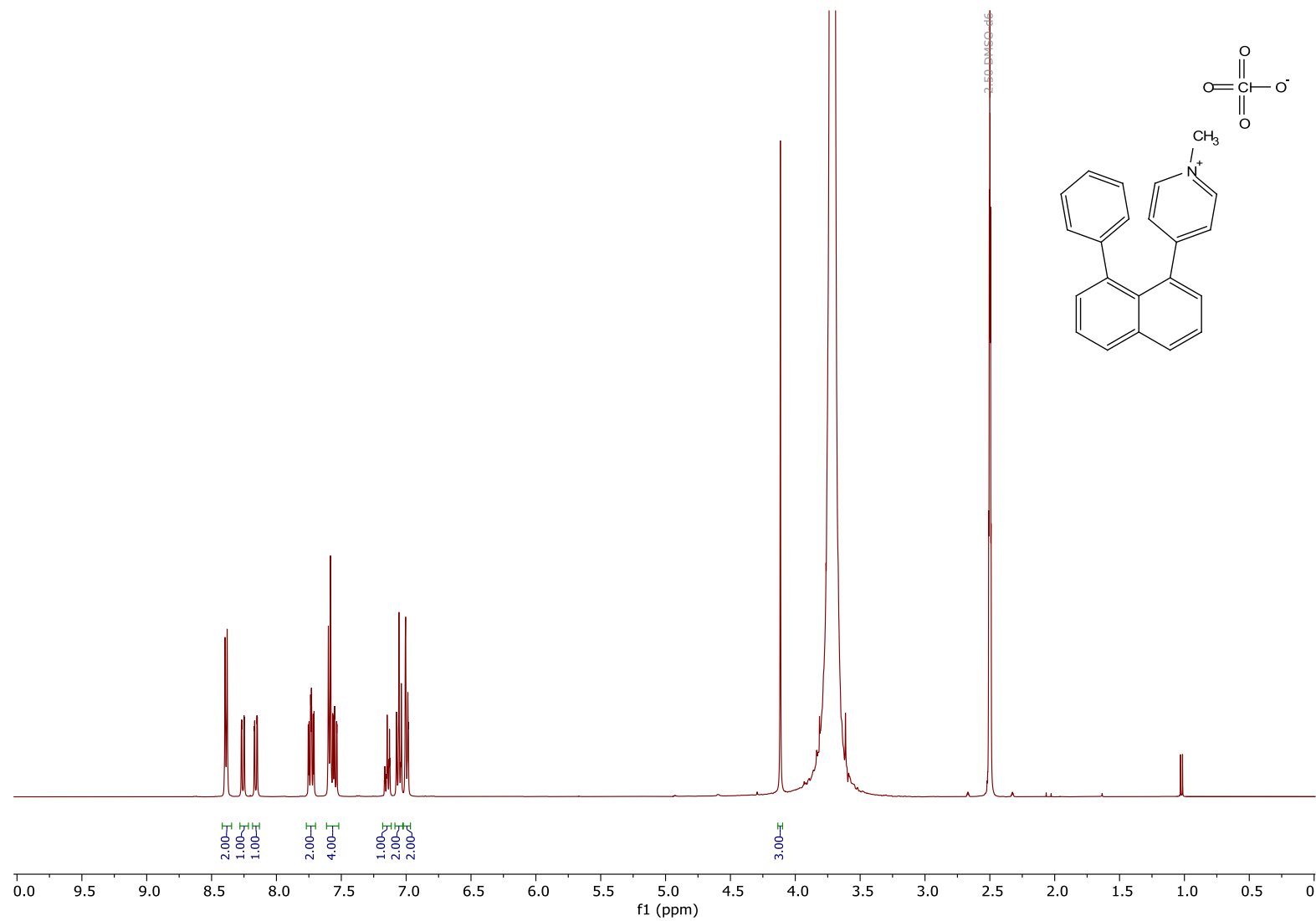
Supporting Information S45

$^{13}\text{C}\{^1\text{H}\}$ NMR (101 MHz, CDCl_3 , ppm) spectrum of 4-(8-Phenylnaphthalen-1-yl)pyridine (**12**)



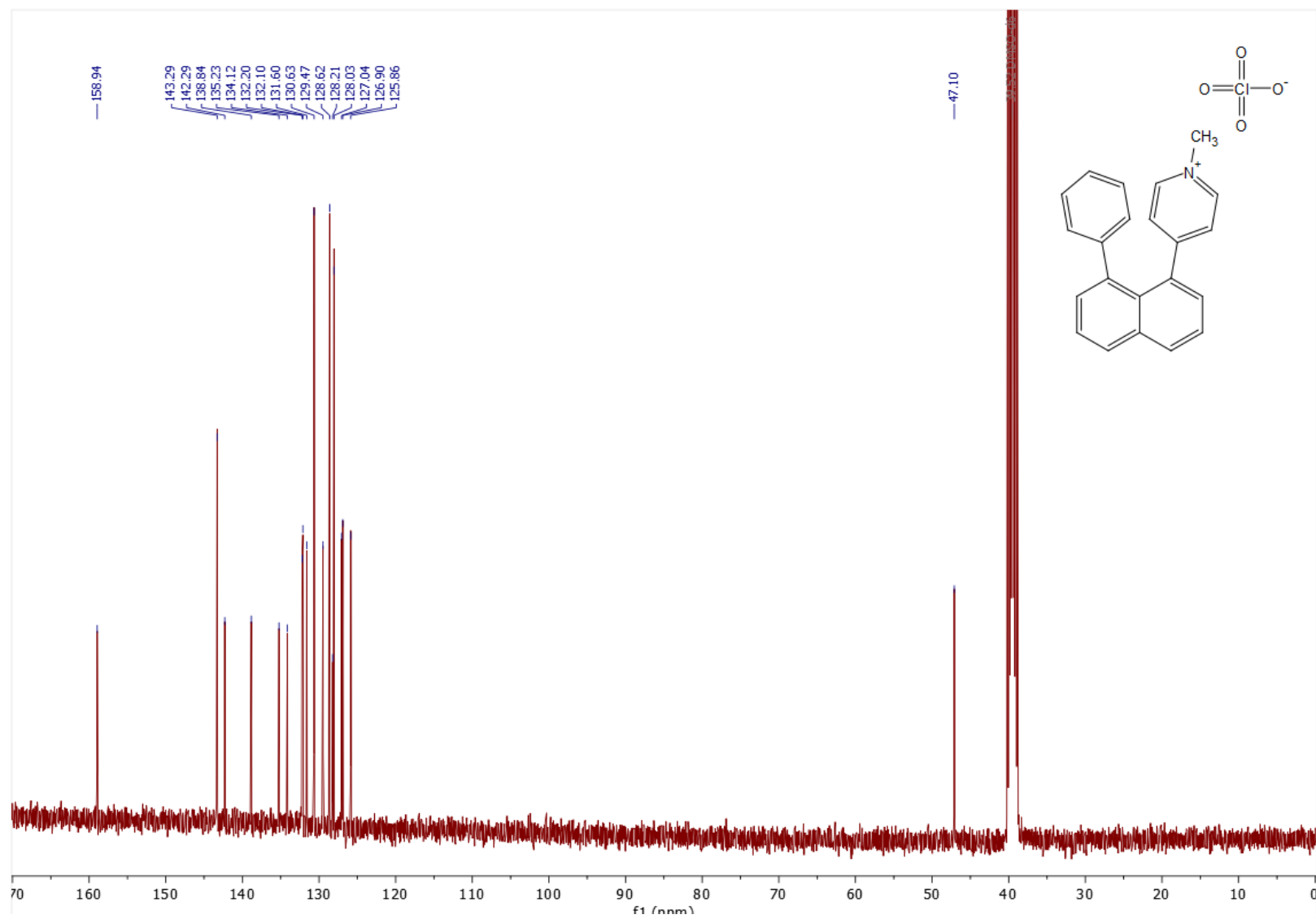
Supporting Information S46

^1H NMR (400 MHz, $(\text{CD}_3)_2\text{SO}$, ppm) spectrum of 1-methyl-4-(8-phenylnaphthalen-1-yl)pyridin-1-ium perchlorate (**2**)

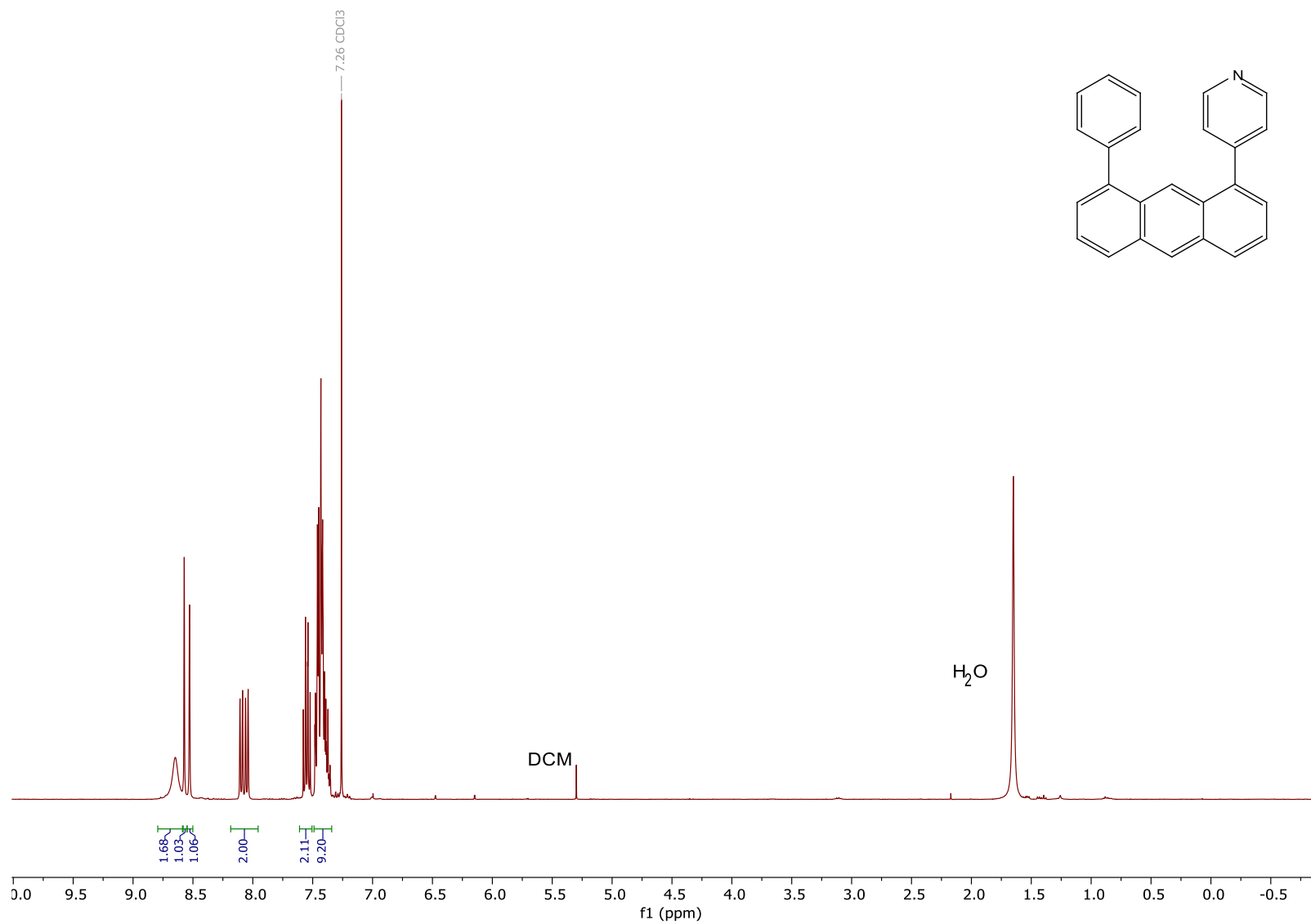


Supporting Information S47

$^{13}\text{C}\{^1\text{H}\}$ NMR (101 MHz, $(\text{CD}_3)_2\text{SO}$, ppm) spectrum of 1-methyl-4-(8-phenylnaphthalen-1-yl)pyridin-1-ium perchlorate (**2**)

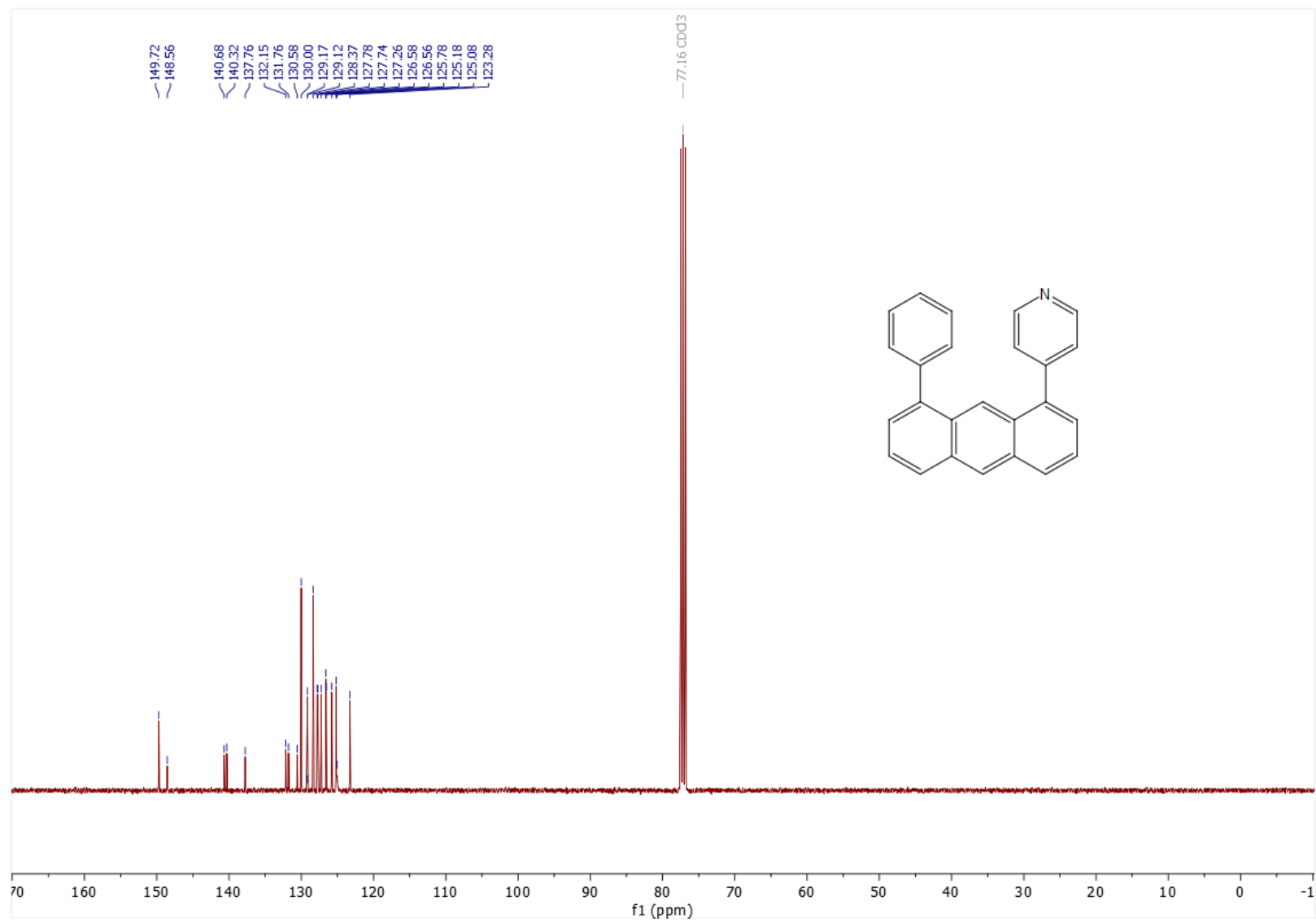


^1H NMR (400 MHz, CDCl_3 , ppm) spectrum of 4-(8-phenylanthracen-1-yl)pyridine (**14**)



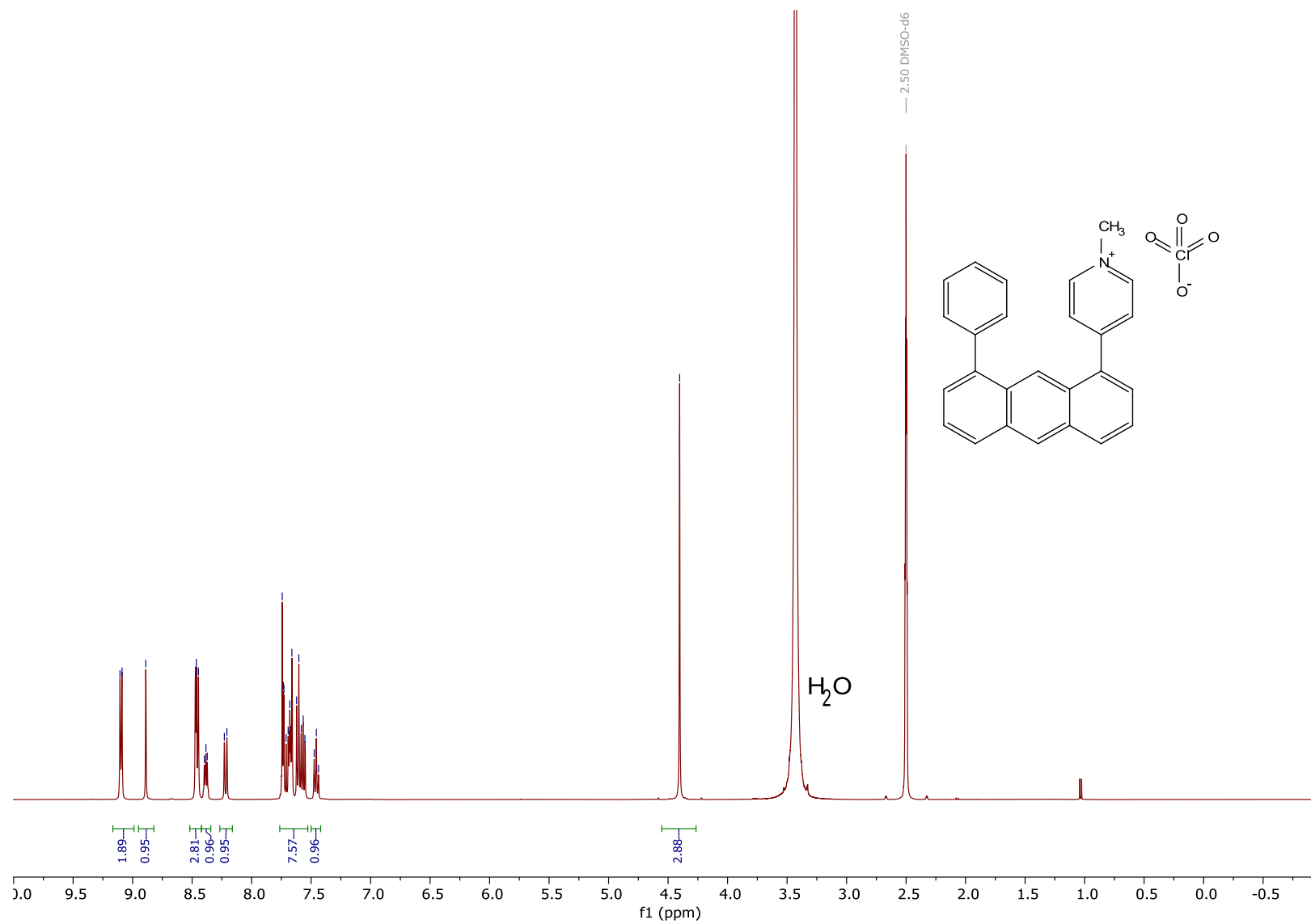
Supporting Information S49

$^{13}\text{C}\{^1\text{H}\}$ NMR (101 MHz, CDCl_3 , ppm) spectrum of 4-(8-phenylanthracen-1-yl)pyridine (**14**)



Supporting Information S50

^1H NMR (400 MHz, $(\text{CD}_3)_2\text{SO}$, ppm) spectrum of 1-methyl-4-(8-phenylanthracen-1-yl)pyridin-1-ium perchlorate (**3**)



Supporting Information S51

$^{13}\text{C}\{^1\text{H}\}$ NMR (101 MHz, $(\text{CD}_3)_2\text{SO}$, ppm) spectrum of 1-methyl-4-(8-phenylanthracen-1-yl)pyridin-1-ium perchlorate (**3**)

